

DETECTION OF NUCLEAR PARTICLE

TRACKS IN FILM

A Thesis

**Submitted to the Graduate Faculty of the
Louisiana State University and
Agricultural and Mechanical College
in partial fulfillment of the
requirements for the degree of**

Master of Science

in

The Department of Nuclear Engineering

by

**Michael T. Pulaski
B.S.M.E., Louisiana State University, 1968
J.D., Louisiana State University, 1971**

May 1972

ACKNOWLEDGMENT

151

The author is truly grateful and indebted to Dr. Frank A. Iddings whose guidance and encouragement made this work possible. The assistance of Dr. Robert C. McIlhenny and Dr. John C. Courtney is also appreciated. A special thanks to Dr. William F. Curry without whose help the graduate course of study would not have been possible.

TABLE OF CONTENTS

	Page
Acknowledgment	ii
List of Tables	iv
List of Figures	v
Abstract	viii
Chapter	
I. Introduction	1
The Problem	1
II. Review of Related Research	2
History	2
Applications	14
III. Theoretical Considerations	21
IV. Experimental	36
Equipment and Apparatus	36
Exposure	36
Development	39
Identification	41
V. Results	44
VI. Conclusions and Recommendations	65
Conclusions	65
Recommendations	65
Vita	67

LIST OF TABLES

TABLE		Page
1	Fission Track Etching Conditions	6
2	Age Results Obtained from Several Minerals	7
3	Track Registration in Various Solids	9
4	Some Methods for Track or Etch Pit Counting	13
5	Table of Results for S. B. Carpenter's Work on the Use of the Nuclear Track Technique to Determine Trace Quantities of Boron and Uranium in Botanical Materials . . .	17
6	Ranking of Materials According to the Measured Sensitivity	30
7	Values of the Critical Rate of Energy Loss for Different Materials	32
8	Exposure Values	63
9	Developing Techniques	64

LIST OF FIGURES

FIGURE	Page
I. Sketch of Device Used by Fleischer, Price, and Walker to Form Fine Holes	18
II. Variation of Energy Loss Rate Versus Energy Per Nucleon for Mica	22
III. Variation of Resistivity and Track Annealing Time with Temperature for a $P_{205} \cdot 5V_{205}$ Glass	24
IV. Schematic View of Ion Displacements As a Result of the Extensive Ionization Along the Path of a Massive Energetic Charged Particle	26
V. Cross-sectional Area Within Which Electrons Will be Given an Energy of at Least ϵ_0 by Various Energetic Charged Particles	34
XVI. VI. Neutron Generator Facility at the Louisiana State University Nuclear Science Center	40
XVII. VII. Photograph of a Stage Micrometer to Verify the Magnification of the Microscope at 430X	43
XVIII. VIII. Photograph of Cellulose Nitrate Film Exposed to a Fast Neutron Flux Shown in the Region to the Side of the Uranium Foil Placement	45
XIX. IX. Photograph of Cellulose Nitrate Film Exposed to a Fast Neutron Flux Beneath the Uranium Foil	45
XX. X. Photograph of Cellulose Nitrate Film Exposed to a Fast Neutron Flux Shown in the Uranium Foil-Film Interface	47
XXI. XI. Photograph of Cellulose Nitrate Film Exposed to a Fast Neutron Flux for Use as a Basis for Flux Reduction Determination	47
XXII. XII. Photograph of Cellulose Nitrate Film Exposed to a Fast Neutron Flux with One Sheet of Aluminum Covering for Particle Flux Reduction (Accidentally Over-etched)	48

FIGURE	Page
XIII. Photograph of Cellulose Nitrate Film Exposed to a Fast Neutron Flux with Two Sheets of Aluminum Covering for Particle Flux Reduction (Accidentally (Over-etched)	48
XIV. Photograph of Cellulose Nitrate Film Exposed to a Fast Neutron Flux with Three Sheets of Aluminum Covering for Particle Flux Reduction	49
XV. Photograph of Cellulose Nitrate Film Exposed to a Fast Neutron Flux with Four Sheets of Aluminum Covering for Particle Flux Reduction	49
XVI(a). Photograph of Cellulose Nitrate Film Exposed to Fast Neutron Flux. Bottom Plate	52
XVI(b). Photograph of Cellulose Acetate Butyrate Film Exposed to a Fast Neutron Flux. Top Plate	52
XVII(a). Photograph of Cellulose Nitrate Film Exposed to a Fast Neutron Flux. Right Plate	53
XVII(b). Photograph of Cellulose Acetate Butyrate Film Exposed to a Fast Neutron Flux. Left Plate	53
XVIII(a). Photograph of Cellulose Nitrate Film Exposed to a Fast Neutron Flux. Top Plate	54
XVIII(b). Photograph of Cellulose Acetate Butyrate Film Exposed to a Fast Neutron Flux. Bottom Plate	54
XIX(a). Photograph of Cellulose Nitrate Film Exposed to a Fast Neutron Flux. Left Plate	55
XIX(b). Photograph of Cellulose Acetate Butyrate Film Exposed to a Fast Neutron Flux. Right Plate	55
XX. Photograph of Cellulose Nitrate Film Exposed to a Fast Neutron Flux in Order to Produce Both Alpha and Proton Tracks	57
XXI. Photograph of Cellulose Nitrate Film Exposed to a Thermal Neutron Flux in Order to Eliminate Alpha Track Production	57
XXII. Photograph of Cellulose Nitrate Film Exposed to a Fast Neutron Flux Beneath the Uranium Foil	58

FIGURE	Page
XXIII. Photograph of Cellulose Acetate Butyrate Film Exposed to a Fast Neutron Flux Beneath the Uranium Foil	58
XXII(a). Photograph of Cellulose Nitrate Film Exposed to a Fast Neutron Flux Showing the Region to the Side of the Uranium Foil Placement	59
XXIII(a). Photograph of Cellulose Acetate Butyrate Film Exposed to a Fast Neutron Flux Showing the Region to the Side of the Uranium Foil Placement	59
XXIV. Photograph of Cellulose Nitrate Film Exposed to a Thermal Neutron Flux Beneath the Uranium Foil	61
XXV. Photograph of Cellulose Acetate Butyrate Film Exposed to a Thermal Neutron Flux Beneath the Uranium Foil	61
XXIV(a). Photograph of Cellulose Nitrate Film Exposed to a Thermal Neutron Flux Showing the Region to the Side of the Uranium Foil Placement	62
XXV(a). Photograph of Cellulose Acetate Butyrate Film Exposed to a Thermal Neutron Flux Showing the Region to the Side of the Uranium Foil Placement	62

ABSTRACT

The results of an investigation to experimentally produce nuclear particle tracks in film is presented. The track-etch technique was used in conjunction with special film coatings on a polyester base utilizing the facilities of the Louisiana State University Nuclear Science Center.

The scope of this work covered only two films - cellulose nitrate and cellulose acetate butyrate. The particles observed were protons, alphas, and uranium fission products from interactions by neutrons produced by a Texas Nuclear Corporation 150 KV Cockcroft-Walton accelerator.

The films were compared for sensitivity to each of the three nuclear particles involved and the results compared favorably with other work done in the same area.

in

emul

for

prod

gate

3) at

part

Louisiana

The

Nuclear

foot

CHAPTER I

INTRODUCTION

The Problem*

In recent years it has been discovered that heavy, charged particles produce submicroscopic tracks in many insulating solids including crystals, inorganic glasses, and plastics. These findings have led to the development of new particle detectors with important advantages over prior detectors in certain nuclear science applications. It has also been found that many solids contain ancient particle tracks which yield information about the history of a sample.

In general, any technique which will enable the solid-state physicist to study particle effects directly is a valuable tool in obtaining a better understanding of the radiation effects in solids. Detectors which permit a permanent recording of nuclear particle tracks in many solids are often superior to the photographic nuclear track emulsions. However, nuclear emulsions have been the principal detector for the past three decades.

The purpose of this work is threefold: 1) experimentally produce visible particle tracks in different materials, 2) investigate a variety of nuclear reactions with regard to hole formation, and 3) study possible application of the accelerator to techniques involving particle tracks using the existing facilities and equipment at the Louisiana State University Nuclear Science Center. Some of these

*The material discussed in this Chapter was taken in part from "Nuclear Track Registration in Solids by Etching" (K. Becker). See footnote 20, page 12.

applications would include low level analysis of fissionable or α -producing materials, production of biological filters, and imaging for neutron radiography.

can

to

but

with

were

be

The

some

would

Price

that

ately

1. Sil

2. Pr

3. Pr

P.

4. Pr

(1

5. Pr

P.



CHAPTER II

REVIEW OF RELATED RESEARCH

History

The tracks to be considered consist of radiation-damaged material produced by the passage of heavy, charged particles. They were first observed in 1959 by Silk and Barnes¹ in mica that had been heavily irradiated with fission fragments. By the use of an electron microscope, damaged linear regions whose diffraction contrast images were approximately 100 Å in diameter were observed.

Price and Walker^{2,3} then found that the tracks in mica could be developed and fixed by immersing the mica in hydrofluoric acid. The acid dissolved the damaged trails and produced permanent channels some 30 to 50 Å in diameter. With prolonged etching, these channels could be enlarged until they became visible in an optical microscope.⁴ Price and Walker then showed that mica could only register tracks that were produced from particles whose mass was greater than approximately thirty atomic mass units.⁵

-
1. Silk, E. C., and R. S. Barnes, Phil. Mag., Vol. 4, p. 970 (1959).
 2. Price, P. B., and R. M. Walker, Physics Review Letters, 8, 217 (1962).
 3. Price, P. B., and R. M. Walker, Journal of Applied Physics, Vol. 33, p. 3407 (1962).
 4. Price, P. B., and R. M. Walker, Physics Letters, Vol. 3, p. 113, (1962).
 5. Price, P. B., and R. M. Walker, Journal of Applied Physics, Vol. 33, p. 3400 (1962).

The track etch technique was then applied to other materials, including glasses⁶ and plastics.⁷ R. L. Fleischer and P. B. Price irradiated various glasses with ^{252}Cf fission fragments, etched in hydrofluoric acid and then examined either optically or electron microscopically. Conical pits were observed in silicate, borate, and phosphate glasses, as well as in natural glass, of both volcanic and extra-terrestrial origin. The detectable length of the trail of damage was measured by etching until the pits became flat-bottomed. It was observed that the etchable length of a fission fragment trail in soda-lime glass was about 11μ , which was somewhat less than the expected maximum range ($\sim 17\mu$). It was also found that the diameter of the pits increases linearly with etching time although they appear to maintain the same cone angle as they enlarge. This cone angle, θ , depends upon the ratio, R , of the chemical attack rate along the damaged material of the track to the general rate of attack of the undamaged material. Long, narrow etch channels may be produced which identify the direction of the damage trail as well as the location of the damage. These phenomena occur also in inorganic glasses and hence are not restricted to crystalline solids. R. Fleischer and P. Price produced pits indicating fission fragment tracks in condensation polymers - bisphenolacetone

-
6. Fleischer, R. L. and P. B. Price, Journal of Applied Physics, Vol. 34, p. 2903 (1963).
7. Fleischer, R. L., and P. B. Price, Science, Vol. 140, p. 1221 (1963).

carbonate, polyethylene glycol terephthalate, cellulose nitrate, cellulose acetate and polymethyl methacrylate using a ^{252}Cf source. They observed that alpha particles emitted by the ^{252}Cf did not lead to observable pits. They also noted that the tracks in the Lexan had a maximum length of about 20 microns which was about their estimated range for the material. The sensitivities varied among the materials, the most sensitive being cellulose nitrate and revealing tracks of α particles⁸ and deuterons.⁹

Work has also been done to develop techniques for geological dating of minerals by chemical etching of fission fragment tracks.¹⁰ Again the work was done using a ^{252}Cf neutron source. Table 1 is a compilation of etching conditions for revealing fission tracks in some minerals studied, including the micas and natural glasses. To date samples by the fission track method, the spontaneous track count (ρ_s) is made, the sample is exposed to a known dose ϕ of thermal neutrons, and a second count is made to find the increase in the track density (ρ_i) due to induced fission. The age A is given by

$$\rho_s / \rho_i = [\exp(\lambda_D A) - 1](\lambda_f / \lambda_D \phi \sigma I)$$

-
8. Fleischer, R. L., P. B. Price, R. M. Walker and E. L. Hubbard, Physics Review, Vol. 133A, p. 1443 (1964).
 9. Fleischer, R. L., P. B. Price and R. M. Walker, Science, Vol. 149, p. 383 (1965).
 10. Fleischer, R. L., and P. B. Price, GEOCHIMICA ET COSMOCHIMICA ACTA, Vol. 28, p. 1705 (1964).

TABLE 1
FISSION TRACK ETCHING CONDITIONS

Mineral	Etch	Time	Temp. (°C)	Crystal plane	Total no. of samples examined	No. known to contain fossil tracks	Remarks
Apatite	HNO ₃	10-30 sec	23	(0001) and (1010)	3	3	Favorable for dating
Barite	HNO ₃	3 hr	100	(001)	2	ε	Shallow pits
Calcite	10% HCl	50 sec	23	(1011)	1	0	Favorable for dating
Glass (natural)	48% HF	5 sec to 4 min	23	--	many	many	
Halite	Ethanol + 3g/l. HgCl ₂	30 sec	23	(100)	1	ε	Shallow pits
Hornblende	48% HF	5-60 sec	23-60	(110)	5	4	Some samples favorable for dating; some have many inclusions and dislocations
Microcline	48% HF	1-10 sec	23	(010)	9	2	Usually too many inclusions and dislocations
Muscovite	48% HF	10-40 min	23	(0001)	~ 50	~ 35	Favorable for dating
Quartz	KOH (aq. sol.) 48% HF	3 hr 24 hr	150 23	(0001) (1010)	4	0	Too few tracks in all samples studied
Topaz	KOH (aq. sol.)	100 min	150	(110) and (100)	1	0	
Zircon	1 part KOH ⁺ 1 part NaOH	10 sec	450	(100)	3	0	Shallow pits

where λ_f = fission decay constant for U^{238}

λ_D = total decay constant

σ = cross-section for thermal neutron-induced fission of U^{235}

I = isotopic ratio of U^{235} to U^{238}

TABLE 2

AGE RESULTS OBTAINED FROM SEVERAL MINERALS

Location	Mineral Type	Fission track age (m.y.)	K-A or Rb-Sr age (m.y.)	Uranium conc. (wt. fraction)
Texas (Llano)	Hornblende	1060 ± 60	~ 1075	~ 0.4.10 ⁻⁶
Norway (Froland)	Hornblende	770 ± 70	not known	0.3.10 ⁻⁶
Ontario (Wilberforce)	Apatite	250 ± 50	~ 1000	~ 100.10 ⁻⁶

During the same period of time that Price and Walker were doing their work with etching techniques, Childs and Silfkin reported the discovery of a decoration method of developing tracks to optical size in single crystals of silver chloride.¹¹

There evolved two general methods to develop the tracks in materials:

- 1) Chemical etching
- 2) Precipitation

and two methods of detecting particles:

- 1) Physical measurements such as gas flow or ionic permeability
- 2) Naked eye observations

11. Childs, C. and L. Silfkin, Physics Review Letters, Vol. 2, p. 254 (1962).

Because of the large free energy associated with a disordered structure, radiation damage trails are generally much more chemically reactive than normal material. If a substance containing damage tracks is immersed in a solvent, those damage trails which intersect a surface are preferentially leached. Tracks which do not intersect a surface are not developed.

Not all tracks which intersect an etched surface will necessarily be revealed. If the general rate of attack perpendicular to the surface is V_G and the velocity of attack along the track is V_T all tracks making an angle less than $\theta_C = \sin^{-1} V_G/V_T$ with respect to the surface will not be seen; the surface dissolves away more quickly than the tracks can be developed.¹²

Track etching in a given substance can be affected by the choice of etchant, its concentration, the orientation of the attacked surface, and the temperature of attack. Table 3 summarizes minimum energy and maximum sensitivity for some recording media.¹³ The chemical and physical pre- and/or post-treatment of the detector material will have an effect on the etching speed.

The most successful application of the precipitation technique has been made by Childs and Silfkin.¹⁴ They decorated tracks throughout the volume of a thick single crystal of silver

-
12. Fleischer, R. L., and P. B. Price, Journal of Geophysical Research, Vol. 69, p. 331 (1964).
 13. Fleischer, R. L., P. B. Price and R. M. Walker, Annual Review of Nuclear Science, Vol. 15, p. 6 (1965).
 14. Childs, C., Op. Cit., p. 4.

TABLE 3

TRACKS REGISTRATION IN VARIOUS SOLIDS

A. Solids for which $(dE/dX)_c$ has been measured
(in order of increasing sensitivity)

Material	Etching Conditions	Critical rate of energy loss (MeV mg ⁻¹ cm ⁻²)	Lightest detectable particle
Olivine	KOH sol'n, 6 min, 160°C; 10% HF, 30 sec, 23°C; 2 to 4 sequences	~ 20	
Hypersthene	NaOH sol'n, 3 to 10 min, 200°C		
Zircon	85% H ₃ PO ₄ , 1 min, 450-500°C	~ 19	~ Ca
Labradorite	KOH sol'n, 15 min, 210°C		
P ₂ O ₅ glass	48% HF, 30 min, 23°C		
Na-Ca glass	48% HF, 3 sec, 23°C		
Tektite glass	48% HF, 30 sec, 23°C	~ 15	~ S
Orthoclase	48% HF, 10 sec, 23°C		
Quartz	KOH sol'n, 10 min, 210°C		
Mica	48% HF, 3 sec-40 min, 23°C	~ 13	Si
Mylar	6N NaOH, 10 min, 70°C		O
Lexan	6N NaOH, 8 min, 70°C	~ 4	C
HBpaIT ^a	6N NaOH, 8 min, 70°C		B
CAB ^a	6N NaOH, 12 min, 70°C		~ He
CN ^a	6N NaOH, 2-4 hr, 23°C	~ 2	H

^aCN = cellulose nitrate; CAB = cellulose acetate butyrate; HBpaIT = polyester of composition C₁₇H₉O₂.

TABLE 3 (cont'd)

B. Solids for which $(dE/dX)_c$ has not been measured
(in alphabetical order)

Material	Etching Conditions
Albite	NaOH sol'n, 4 min, 195°C
Anorthite	KOH sol'n, 30 min, 210°C
Apatite	70% KNO ₃ , 10-30 sec, 23°C
Augite	KOH sol'n, 1 min, 220°C
Autunite	10% HCl, 10-30 sec, 23°C
Barite	70% HNO ₃ , 3 hr, 100°C
Beryl	KOH sol'n, 9 hr, 150°C
Bronzite	NaOH sol'n, 6 min, 200°C
Bytownite	KOH sol'n, 15 min, 210°C
Calcite	10% HCl, 1 min, 23°C
Cerussite	100% HAc, 10-30 min, 23°C
Diopside	KOH sol'n, 15 min, 210°C
Enstatite	NaOH sol'n, 15 min, 195°C
Fluorite	98% H ₂ SO ₄ , 10 min, 23°C
Garnet	KOH sol'n, 2 hr, 150°C
Glasses	10-48% HF, 1 sec-30 min, 23°C
Gypsum	5% HF, 5-10 sec, 23°C
Halite	Ethanol + 3g/l HgCl ₂ , 30 sec, 23°C
Hornblende	48% HF, 5-60 sec, 23-60°C
Layer-structure Silicate minerals	48% HF, 3 sec to 40 min depending on mineral, 23°C
Microcline	48% HF, 1-10 sec, 23°C
Pigeonite	KOH sol'n, 15 min, 210°C
Spodumene	48% HF, 24 hr, 23°C
Thorite	85% H ₃ PO ₄ , 1 min, 250-300°C
Topaz	KOH sol'n, 100 min, 150°C
Torbernite	10% HCl, 10 min, 23°C
Tourmaline	KOH sol'n, 20 min, 220°C
Tridymite	10% HF, 60 min, 23°C
Whitlockite	70% HNO ₃ , 10 sec, 23°C

chloride using a combination of pulsed light and electric fields to sweep photoelectrons into the interior of the crystal. The silver chloride crystals have the following advantages over emulsions:

- a) the development may be quicker, b) there is no distortion in the development process so that accurate angle measurements are possible,
- c) the crystals are insensitive to lightly ionizing particles; and
- d) the density is about twice that of emulsions. Although the electron injection technique is probably applicable to other silver salts it was found not to be applicable to most crystals. The standard methods of decorating involving heating and subsequent quenching are probably not very effective since the tracks may anneal out during the heating period.¹⁵

It has been suggested that the number of tracks can be determined by physical measurements such as gas flow or ionic permeability, thereby eliminating the use of a microscope.¹⁶ Bean, Doyle, and Entine have obtained reproducible curves of all conductivity as a function of time using an irradiated mica specimen as a barrier between two halves of a cell containing an HF solution.¹⁷ Mory and Walker however were unable to obtain satisfactory results using irradiated plastics as the cell membrane.¹⁸

-
15. Amelinckx, S., Solid State Physics, Supp. 6 (1964).
 16. Fleischer, R. L., P. B. Price and R. M. Walker, Applied Physics Letters, Vol. 3, p. 28 (1963).
 17. Bean, C. P., M. V. Doyle, and G. Entine, (To be published).
 18. Mory, J., and R. M. Walker, Fifth International Conference of Nuclear Photography, (CERN, 1964).

In another type of track detection an opaque coating of aluminum was applied to one side of a plastic sheet, which was then relative to the length of the tracks being detected. The plastic is subsequently etched from the uncoated side. At track locations, the hydroxide solution flows through and attacks the aluminum film. In a short time each microscopic track is surrounded by a relatively large, easily visible circular area from which the aluminum has been removed.¹⁹

Most quantitative work using solid-state particle detectors requires the determination of the number of etch pits per unit area of detector surface. Visual counting is slow and tedious and therefore automatic procedures are desirable. Table 4 lists some counting techniques which are used.²⁰

Recently, Metals Research Company has developed a new method of image analysis utilizing mechanical optical scanners and a computer which can scan the field of tracks and perform programmed calculations based upon the information received from the scanner.²¹

Most of the research considered in this section dealt with heavy particle accelerators and exposures obtained from reactors. However, the author was fortunate enough to have obtained a copy of

-
19. Fleischer, R. L., P. B. Price, and R. M. Walker, Annual Review of Nuclear Science, Vol. 15, p. 7 (1965).
 20. Becker, K., "Nuclear Track Registration in Solids by Etching," Biophysik, Vol. 5, pp. 207-222 (1968).
 21. Cole, Michael, "Image Analysis," American Laboratory, June 1971, p. 19.

TABLE 4

SOME METHODS FOR TRACK OR ETCH PIT COUNTING

Microscopic Techniques	Macroscopic Techniques	
	for low track densities	for high track densities
1. Visual counting	1. Dye penetration through holes in membranes	1. Optical density
2. Flying spot scanning	2. Light penetration through one-side aluminized thin foils	2. Light scattering at etched surface
3. Measurement of scattered light in dark-field microscope	3. Electric discharges (sparks) through holes	3. UV-penetration through perforated foils
a) Pulse-counting type b) Integral intensity		4. Dielectric constant of perforated foil
		5. Electrolyte penetration through perforated foil

research done recently by Harold Berger of Argonne National Laboratory²² in which he experimented with different techniques for image detection for 14.5 MeV neutrons. H. Berger attempted three methods for detecting images:

- 1) the direct method,
- 2) the transfer method, and
- 3) the track-etch method.

This last method is of great importance for the present investigation since the procedures and materials used by H. Berger are essentially the ones under consideration by the author. H. Berger concluded that of three plastics chosen for the detection medium, the cellulose nitrate was superior in terms of both sensitivity and contrast. The cellulose nitrate was compared with polycarbonate plastics Lexan (manufactured by General Electric) and Makrofol Types E and N (manufactured by Bayer A.G.).

Applications

One of the largest areas of application of track detectors is in nuclear physics research. Mica sandwich detectors were used at Brookhaven and at CERN to study the energy and mass dependence of high energy fission.^{23,24} Burnett and others have used mica detectors

-
22. Berger, Harold, "Image Detection Methods for 14.5 MeV Neutrons: Techniques and Applications" (unpublished).
 23. Fleischer, R. L., P. B. Price and R. M. Walker, Annual Review of Nuclear Science, Vol. 15, p. 14 (1965).
 24. Brandt, R., C. Gfeller, and J. Zakrzowski, CERN Preprint No. 64-49 (1964).

to measure the fission cross section of the compound nucleus Tl^{201} produced by the bombardment of high purity Au^{197} with He ions in the Berkeley 88-inch cyclotron.²⁵ The spontaneous-fission decay constant of U^{238} has been determined by measuring the track densities in a mica sheet placed next to a uranium foil for six months and in a piece of uranium-rich glass of known manufacture date.²⁶

Solid-state track detectors also make it possible to measure both the concentration and distribution of elements such as uranium and thorium which fission under neutron exposure;^{27,28} and of elements such as boron which has a large (n,α) cross-section.²⁹ S. Thomas Elleman and Donald C. Kesler of North Carolina State Univ. (NCSU) have used glass slides and the etch-pit technique in uranium detection.²⁸ Standard glass microscope slides were placed in contact with uranium bearing specimens and irradiated with thermal neutrons in the NCSU reactor. The slides were etched in 48% hydrofluoric acid, neutralized in 10% ammonium hydroxide and rinsed in running water. They observed that the etch-pit background (due to spontaneous fission of uranium impurities in the glass as well as to the registration of cosmic-ray

26. Fleischer, R. L., and P. B. Price, Physics Review, Vol. 133, B63 (1964).

27. Price, P. B., and R. M. Walker, Applied Physics Letters, Vol. 2, p. 23 (1963).

28. Elleman, T. S., and D. C. Kesler, "Application of Fission-Fragment Etch-Pit Techniques in Uranium Detection," Nuclear Applications and Technology, Vol. 7, August 1969.

29. Carpenter, S. B., "The Use of the Nuclear Track Technique for Boron and Uranium Analyses in Botanical Material,"

events) imposed detection limitations on the use of glass in the detection of small uranium concentrations or as a low-fluence radiation dosimeter. When used as a dosimeter, the glass was contacted with a natural or enriched uranium foil. It was found that the enriched foil dosimeter would have a threshold sensitivity of $\sim 5 \times 10^4$ n/cm² or a thermal-neutron flux threshold of ~ 0.6 n/cm²-sec for a one day exposure. It was also observed that there were pronounced inhomogeneities in uranium distribution in U-doped CsI single crystals. Crystals grown by pulling were observed to have high uranium concentrations along the center axis while those grown by recrystallization inside a quartz tube exhibited high surface concentrations. T. Elleman and D. Kesler also used the glass slide etch-pit technique to detect uranium sputtered from surfaces during the fission process by the use of an aluminum catcher. They observed that the sputtered uranium is not homogeneously distributed as was first expected. It should be noted that their conclusion of glass slide superiority in uranium detection was based upon a comparison with alpha-particle autoradiography in nuclear track plates and was not compared with the cellulose nitrate or polycarbonate films.

Stephen B. Carpenter of the National Bureau of Standards has used the nuclear track technique to determine trace quantities of boron and uranium in botanical materials non-destructively. The ground botanical material was dried in a 90°C oven for 24 hours. After drying, boron and uranium analyses were made in two ways, absolute determination

for both material and the method of standard additions for orchard leaves. The leaves were weighed and pressed into uniform pellets. The pellets were then bonded to detectors, polycarbonate for uranium and cellulose acetate butyrate for boron using melted paraffin. The combination was irradiated in a thermal-neutron flux, of approximately 1.2×10^{13} n/cm²-sec. After irradiation the detector was separated from the sample and etched in 6.5N NaOH. The table below gives the results obtained by S. Carpenter.²⁹

TABLE 5

Absolute Method		
	Boron	Uranium
Orchard leaves	24.11 ± 0.45 ppm	28.19 ± 1.78 ppb
Kale	25.29 ± 0.10 ppm	36.83 ± 1.83 ppb
Method of Standard Additions		
Orchard leaves	24.08 ± 0.32 ppm	26.94 ± 2.37 ppb

The ability to chemically etch out the damage trails in the detector material has also led to the use of track detectors as a means for making sieves. The tracks may be aligned by employing a collimated beam of particles. A simple collimated source of particles is obtained by separating a uranium source from the target, evacuating the intervening space, and exposing the assembly to thermal neutrons. The larger the separation and the smaller the source area, the more

complete will be the resulting hole alignment. Below is a sketch of a device used by Fleischer, Price, and Walker to form these fine holes.³⁰

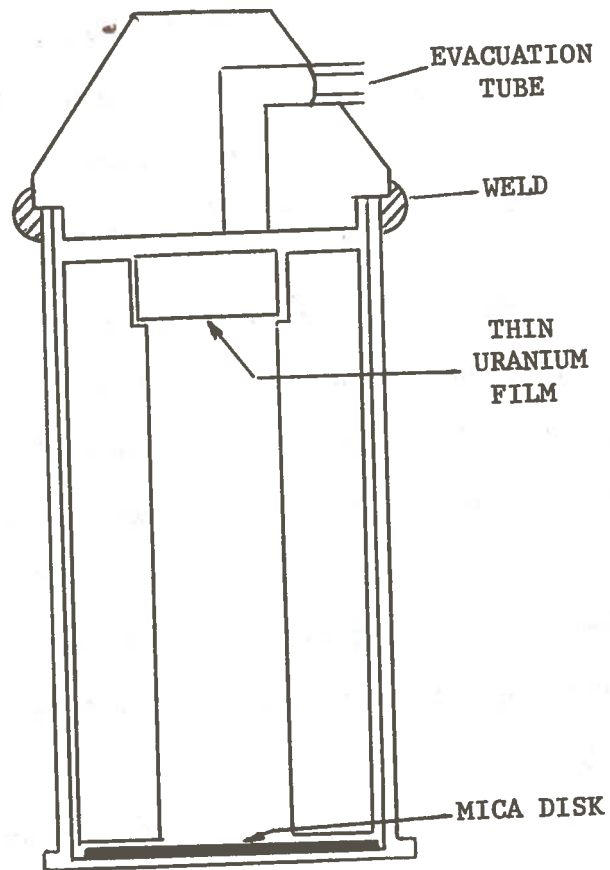


FIGURE I

30. Fleischer, R. L., P. B. Price, and R. M. Walker, "Method of Forming Fine Holes of Near Atomic Dimensions," Review of Scientific Instruments, Vol. 34, Number 5, May 1963, p. 510.

The density of the holes, ρ , was calculated from the following equation:

$$\rho = n\sigma I N_0 t F$$

where n = thermal neutron dose

σ = thermal neutron cross-section for U^{235} fission

I = isotopic abundance of U^{235}

N_0 = the number of U atoms per cm^2 of source

t = the thickness of source (cm)

F = geometrical factor (1/70 for the above setup)

They found that for a 5000 Å pure U^{235} source used in the arrangement above, a density of $\sim 10^{11}$ aligned holes/ cm^2 would require an exposure of ~ 10 minutes in the Brookhaven reactor (flux level $\sim 10^{13}$ mv).

The sieves have been used as a means of separating cancer cells from other cells in the blood.³¹

Another area for application is in personnel dosimeters.

K. Becker³² and others have designed a simple neutron personnel dosimeter which consists of a combination of a small glass plate or plastic foil and a natural uranium foil encased in a cadmium capsule to avoid oversensitivity to thermal neutrons. Such a dosimeter was

31. Seal, S. H., "A Sieve for the Isolation of Cancer Cells and Other Large Cells from the Blood," Cancer (May 1964).

32. Becker, K., Biophysik, Vol. 5, p. 218 (1968).

found to be reasonably energy-independent for neutron energies above 2 MeV but was less sensitive to thermal and intermediate energy neutrons.

In a very recent study by G. M. Comstock and others, it was found that the cosmic ray tracks in the Lexan polycarbonate helmets worn by Apollo 8 astronaut James Lovell and the Apollo 12 astronauts indicate additional shielding may be needed for lengthy deep-space missions.³³

33. Comstock, G. M., et. al., Chemical and Engineering News, p. 10 (April 19, 1971).

CHAPTER III

THEORETICAL CONSIDERATIONS

Each track-detecting material is characterized by a critical value of energy loss rate $(dE/dX)_c$. Particles which give up their energy appreciably less rapid than the critical value do not produce etchable tracks while those depositing appreciably more energy per unit distance register with unit efficiency.

Figure II indicates the results of experiments to measure a value of $(dE/dX)_c$.³⁴ The curves are calculated relations for the variation of energy loss rate with energy for various heavy ions in muscovite mica. The mica was bombarded with heavy ions of various energies and the observations after etching recorded in the graph. The label N indicates that no tracks were etched; L corresponds to long tracks having been observed with unit efficiency; and P signifies partial or incomplete track registration. The figure shows that the efficiency varies from zero to unity over a rather narrow band of energy loss rates.

In the above way, $(dE/dX)_c$ values have been found for a number of materials.³⁴ Other $(dE/dX)_c$ values have been placed in the sequence of their sensitivities by bombardments with high-energy

³⁴. Fleischer, R.L., Price, P.B., Walker, R.M., and Hubbard, E.L., Physics Review, Vol 133A, p. 1443 (1964).

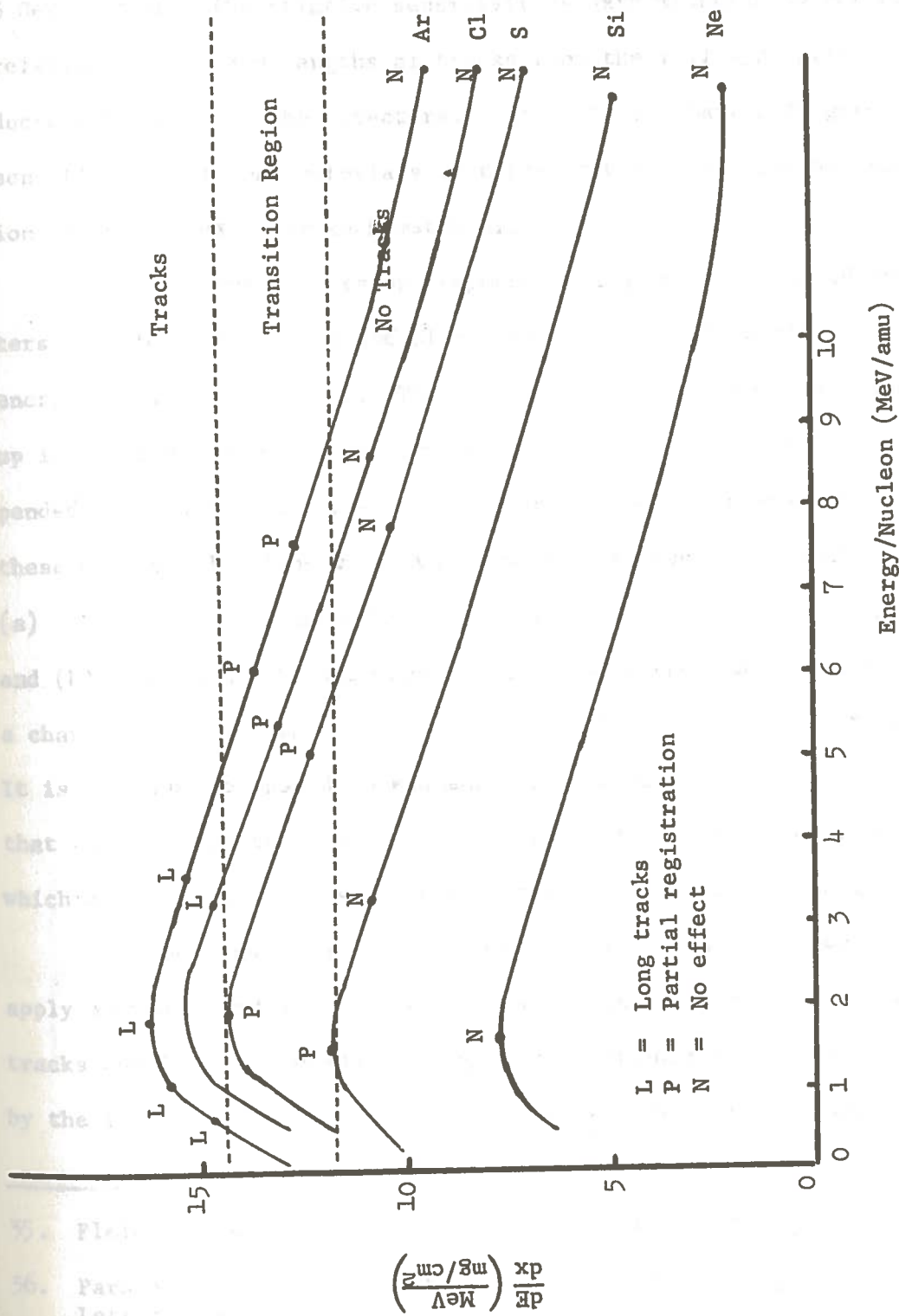


Figure II. Variation of Energy Loss Rate Versus Energy Per Nuclear for Mica.

protons.³⁵ In these experiments, foils of Ag, Nb, Zn, Cu, or Fe were placed in front of the material of interest and then irradiated with 3 GeV protons. The relative sensitivities were measured by noting the relative numbers and lengths of tracks from the foil spallation products which entered the detectors. Table III in Chapter II gives the sensitivities of some materials in terms of both the lightest detectable ion and of $(dE/dX)_c$ for each material.

An energetic fission fragment moving through a solid encounters a collection of ions and of electrons. Such a fragment loses energy in two primary ways. The greater portion of the energy is given up in exciting and accelerating electrons, a lesser amount being expended in elastic interactions with ions. Atomic displacements due to these direct collisions with atoms are not the cause of tracks since (a) they would be expected to occur equally in conductors or insulators, and (b) they would become more prevalent near the end of the range of a charged particle (where it is found that tracks often do not register). It is not implied that displacement spikes never can occur, but merely that they are not the usual cause of tracks in solids. Dot-like defects, which are very likely displacement spikes, have been seen in germanium.³⁶

Again one alternative source of tracks can be shown not to apply generally — the direct effect of displaced electrons. If the tracks consisted of merely the region containing the electrons displaced by the incident charged particle, one would expect that subsequent

35. Fleischer, R. L., Price, P. B., and Walker, R. M., Science (1965).

36. Parsons, J. R., Balluff, R. W., Koehler, J. B., Applied Physics Letters, Vol. 1, p. 59 (1962).

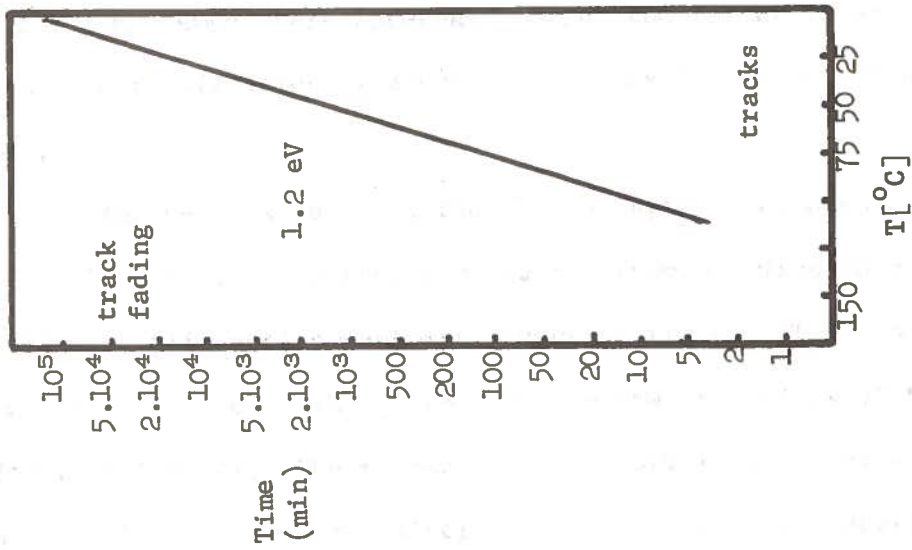
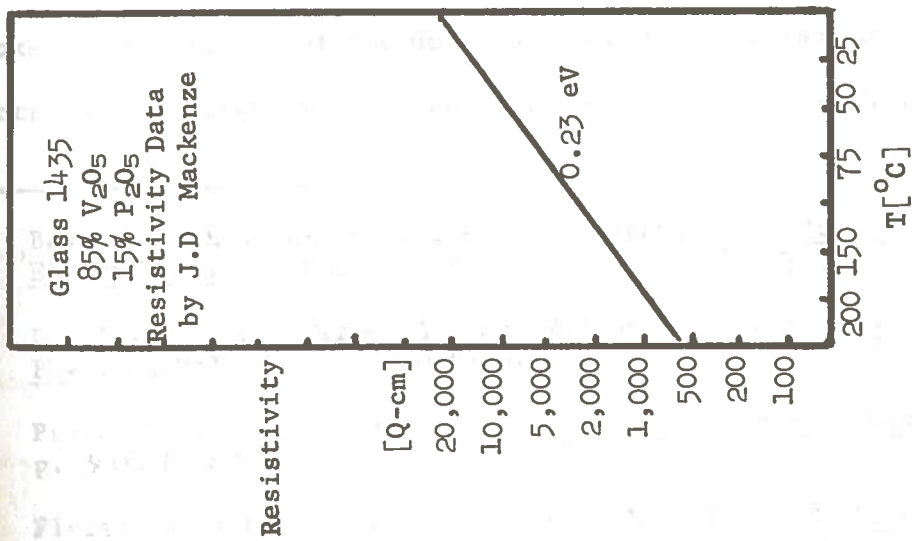


Figure III. Variation of resistivity and track annealing time with temperature for a P₂O₅·5V₂O₅ glass

migration of electrons through the solid would allow them either to diffuse away or to return to their vacated sites. In either case the track would be erased. Figure III shows the result of such a diffusion experiment for a $P_2O_2 \cdot V_2O_5$ glass, which is known to be semiconducting.³⁷ Compared was the activation energy for motion of electrons (derived from the conductivity) with the activation energy for erasing tracks found over the same temperature interval. Since the former is about one-fifth of the latter, migration of electrons by itself does not dissipate tracks.

Another possibility, the thermal spike, has been considered. Bonfiglioli, et al.,³⁸ reported a variation from one mica to another in the width of diffraction contrast images of tracks. They concluded that the width correlated with the relative thermal stability of the different materials. Their observation, however, is in disagreement with Fleischer, Price, and Walker on micas³⁹ and other materials.⁴⁰

Fleischer, Price and Walker suggest an alternative mechanism:⁴¹ Tracks are the result of the defects created by the removal of the electrons. A narrow cylinder which is densely filled with excess

-
37. Baynton, P.L., Rawson, H., and Stanworth, J.E., Journal of Electrochemistry Society, Vol. 104, p. 237 (1957).
 38. Bonfiglioli, G., Ferro, A., and Mojoni, J., Journal of Applied Physics, Vol. 32, p. 2499 (1961).
 39. Price, P. B., and Walker, R. M., Journal of Applied Physics, Vol. 33, p. 3400 (1962).
 40. Fleischer, R.L., Price, P.B., and Walker, R.M., Science, Vol. 149, p. 383 (1965).
 41. Fleischer, R.L., Price, P.B., and Walker, R.M., Journal of Applied Physics, Vol. 36, p. 3645 (1965).

positive ions is thereby created. These positive ions strongly repel one another and are ejected into interstitial positions surrounding a now depleted core region. Figure IV is a schematic diagram indicating

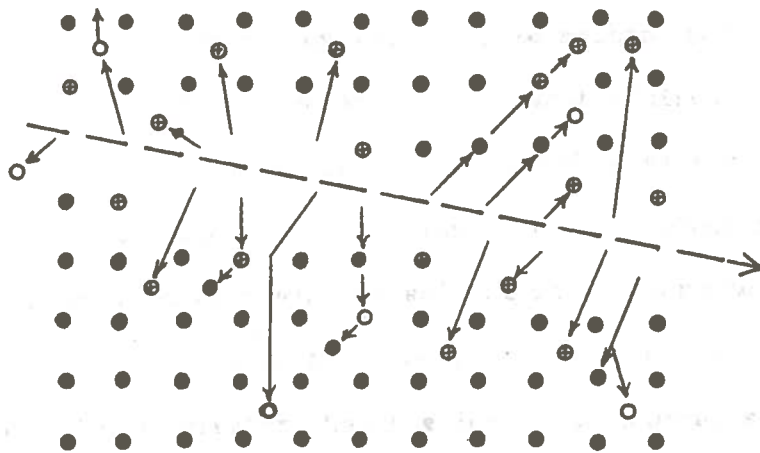


Figure IV. Schematic view of ion displacements as a result of the extensive ionization along the path of a massive energetic charged particle.

the resultant ion displacements, but not the elastic strains and other readjustments which would follow. The process envisioned here is in essence a multiple Varley process,⁴² consisting in this case of a

42. Varley, J.H.O., Nature, Vol. 174, p. 886 (1954).

great many ions mutually repelling one another to create many displacements rather than one displacement pair, such as Varley imagined. The massive defect imagined here is the result of a process similar to the one invoked by Stiegler and Noggle⁴³ as a means of producing fission track grooves at free surfaces of thin metal films. They imagined electrons to be ejected from the metal and to be followed by the ions thereby created.

Now considered are four necessary conditions for the creation of tracks by the ion explosion spike mechanism.⁴¹ To decide what measurable physical parameters are relevant Fleischer, Price and Walker propose an approximate, semiquantitative model for track formation. The model describes the condition that the Coulomb repulsive forces within the ionized region be sufficient to overcome the lattice bonding forces. They express this condition in terms of a local electrostatic "stress" being greater than the local "mechanical strength" or bonding strength. If two ions in a material of dielectric constant ϵ and average atomic spacing a_0 have received an average ionization of n unit charges e , the force between them is $n^2 e^2 / \epsilon a_0^2$, or a local force per unit area (the electrostatic stress σ_e) of $n^2 e^2 / \epsilon a_0^4$. They find what is essentially the interatomic bonding force, in terms of a macroscopically measurable quantity, by noting that the theoretical mechanical tensile strength σ_M of material of Young's modulus E is approximately $0.1E$. It is then seen that the electrostatic stress will be larger than the mechanical strength if $n^2 e^2 / \epsilon a_0^4 > 0.1E$ or if

43. Stiegler, J.O. and Noggle, T.S., Journal of Applied Physics, Vol. 33, p. 1894 (1962).

$$n^2 > R \equiv E\epsilon_0^4/10e^2, \quad (1)$$

where the quantity R defined in (1) is called the stress ratio and will be used later to calculate the relative sensitivity of various track-storing materials.

Relation (1) indicates that tracks should be formed most easily in materials of low mechanical strength, low dielectric constant, and close interatomic spacing.

A second criterion is that in some materials, tracks must be atomically continuous. This requires at least one ionization per atom plane crossed by the incident charged particle. Therefore, $n > 1$ is a second criterion for track formation in such materials. In other materials it is likely that n will be about unity. This limits the investigation to tracks which can be identified by the etching technique. For other methods of revealing tracks different criteria will no doubt apply.

The third requirement for track formation relates to the supply of electrons near an ionized track. If other electrons were able to replace those ejected by the energetic charged particle before the ionized atoms are forced into the adjacent material, no track would result. Thus in order to suppress track formation it would be necessary to drain electrons from a cylindrical region around the ionized track in less time than the 10^{-13} sec needed for the ions to be displaced from their sites. If the density of free electrons is n_n and the number of ionizations/atomic plane is n_a , the radius of the region to be drained is given by

$$\pi r^2 a_0 n_n = n_a \quad (2)$$

The time for electrons to diffuse a distance r is r^2/D , where the diffusion constant D is given by the Einstein relation $\mu_n kT/e$, k being Boltzmann's constant and μ_n the electron mobility. Thus tracks may not be formed unless

$$n_n < e n_a / \pi a_0 \mu_n k T t. \quad (3)$$

For a diffusion time t of about 10^{-18} seconds (a lattice vibration time) it is found⁴¹ that under typical conditions this relation is obeyed by semiconductors and insulators. It does, however, imply that tracks will not form in metals unless the density of conduction electrons were less than, $10^{20}/\text{cm}^3$.

The fourth criterion is set by the mobility of holes. Since the ionized region along a track is in essence a high concentration of holes, they might move away and thereby suppress permanent track formation. If it is assumed that in order to do this holes must diffuse at least one atom distance, then the hole mobility μ_p must be more than $a_0^2 e / t k T$ for track formation to be prevented. This relation requires that at room temperature tracks will not appear in materials whose hole mobility is more than $0.2 \text{ cm}^2/\text{V-sec}$. It follows that metals and many semiconductors, including silicon and germanium, are normally not track storing materials.

The primary criterion for track formation, that the stress ratio R be less than the square of the ionization per atom n^2 , should

Table 6

Ranking of Materials According to the Measured Sensitivity

Material	Critical rate of energy loss
Olivine	$\sim 20 \text{ MeV/mg/cm}^2$
P ₂ O ₅ -glass	$\sim 15 \text{ MeV/mg/cm}^2$
Soda lime glass*	
Tektite glass*	
Mica (18)	$\sim 13 \text{ MeV/mg/cm}^2$
Polyester resin (Mylar) [†]	$\sim 4 \text{ MeV/mg/cm}^2$
Bisphenol-A polycarbonate resin (18) (Lexan) [‡]	
HBpaIT polyester*	
Cellulose acetate butyrate	$\sim 2 \text{ MeV/mg/cm}^2$
Cellulose nitrate (18)	

*Believed to be in this position relative to the other materials

[†]A registered trademark of E.I. Du Pont

[‡]A registered trademark of General Electric

lead to a ranking of materials according to the measured sensitivity, which is presented in Table VI. As R decreases, the sensitivity should increase.

Values of n^2 will depend on the ionization energies of the material and upon the energy and charge of the incident, track-forming particle. Since the ionization energies are a weighted average which will not vary greatly in comparing most materials. At this time variations in n among different materials will be neglected.

In Table VII are listed values of R and of the constants which were used to find R .⁴¹ In cases where values of E were not available in the literature they were measured at a frequency of one KHz. Values of b were obtained as the cube root of the average atomic volume, including all atoms in the structure. In many cases the elastic moduli are not available; hence a second column in which there is calculated a second stress ratio R_h using (in place of $0.1E$) hardness values h , which generally increase with elastic moduli. Indentation hardness numbers were converted to diamond Knoop hardness values.

It can be seen that the values of R separate the materials into four groups - the very sensitive materials, all of which are high polymers; two groups of intermediate sensitivity, the micas and a group which includes inorganic glasses; and the materials of lowest sensitivity such as zircon and olivine. Within the estimated accuracy of the calculated R values there are no exceptions to the regular correlation of R with the critical rate of energy loss.

In order to satisfy the second criterion for track formation, it is necessary to show that a reasonable concentration of ionized atoms

Table 7

Values of the Critical Rate of Energy Loss for Different Materials

Material	R(+50%)	R _n (±50%)	E(10 ¹¹ cgs)	Knoop hardness (10 ¹⁰ cgs)	Dielectric		Composition
					tric	stant	
Olivine	2.6	1.7	10.3	7.0	20		MgFeSiO ₄
Phosphate glass	---	0.4	---	2.8	14		63P ₂ O ₅ :11UO ₂ :8Al ₂ O ₃ :9Ag ₂ O:9K ₂ O
Soda lime glass	1.0	0.4	7.0-7.8	3.2	9		67SiO ₂ :14Na ₂ O:14CaO:5Al ₂ O ₃
Tektite glass	0.7	0.3	7.0	3.4	6.4		72SiO ₂ :12Al ₂ O ₃ :4FeO + others
Muscovite mica	---	0.03	---	0.45	5.7-8.7		KAl ₃ Si ₃ O ₁₀ (OH) ₂
Polyethylene terephthalate	0.02	---	0.45	---	3-6		C ₁₉ H ₁₆ O ₇
Bisphenol-A polycarbonate	0.007	0.008	0.22	0.25	3.1		C ₁₆ H ₁₄ O ₃
HBpaIT polyester	0.013	0.014	---	---	4		C ₁₇ H ₈ O ₂
Cellulose acetate butyrate	0.009	0.009	0.04-0.24	0.20	3.2-6.4		C ₂₀ H ₃₂ O ₅
Cellulose nitrate	0.02	0.02	0.1-0.3	0.25	6-8		C ₅ H ₉ O ₉ N ₂

will be produced along the path of a track-forming charged particle. As noted previously, n must be at least unity for the model presented to be plausible in materials such as mica.

Ozeroff⁴⁴ notes that if a fission fragment of effective charge Z^* , mass M , and energy E_F passes a distance b from an electron, the electron will be given an energy ϵ_e from the equation

$$\epsilon_e = 4mE_F/M(1 + 4b^2m^2E_F^2/M^2Z^{*2}e^4). \quad (4)$$

where e and m are the electronic charge and mass.

Equation (2) has been used⁴⁴ to calculate the electron energy as a function of the electrons' initial separation from the path of several charged particles of interest: full energy light fission fragments, 30 MeV light fission fragments, 160-MeV argon ions, 3-MeV α particles, and 1-MeV particles. Figure V shows these data plotted as an excitation function, where the ordinate πb^2 is the area within which each electron is given at least an energy given by the abscissa. Thus if πb^2 is chosen to be the average atomic cross sectional area, and an energy is computed that is at least as large as the first ionization potential, there will exist a continuous trail of ionization; and one of the requirements for track formation in materials such as mica will be satisfied.

44. Ozeroff, J., USAEC Report AECD 2973 (KAPL Report 205, June 29, 1949).

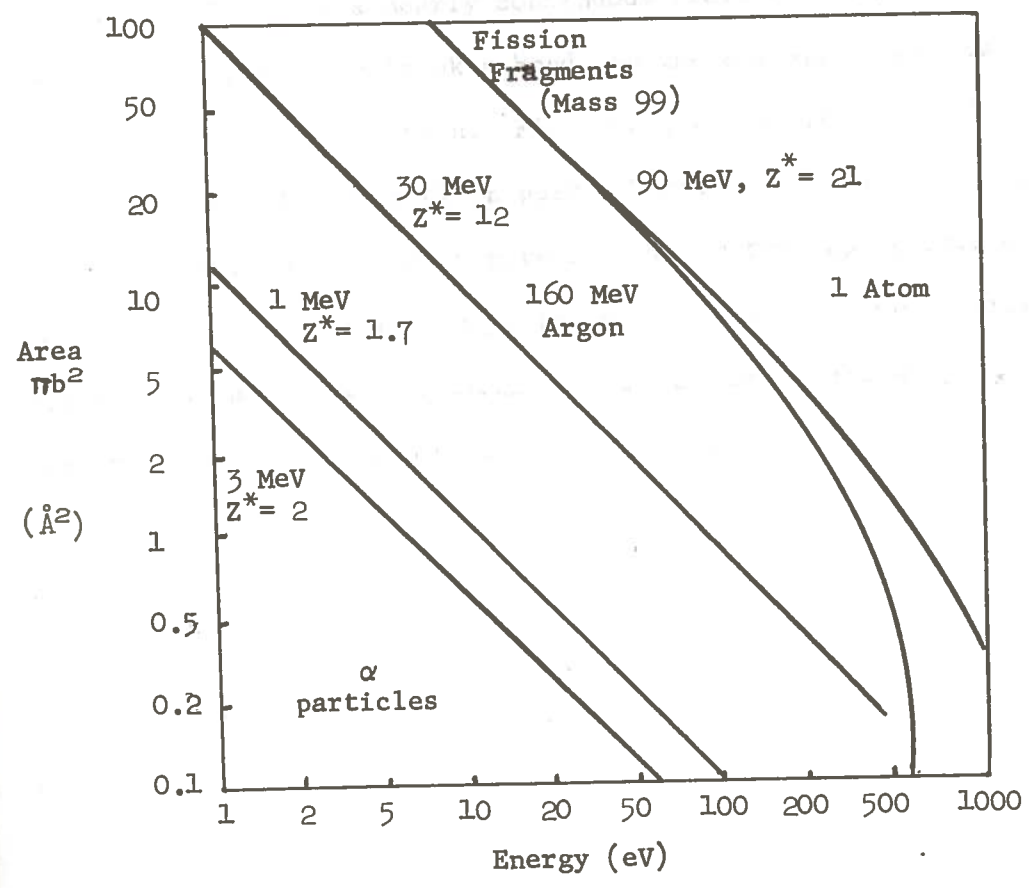


Figure V. Cross-sectional area within which electrons will be given an energy of at least ϵ_{σ} by various energetic charged particles.

In the case of the high polymers, which are the only materials found in which etching reveals tracks of α particles and lighter particles, it is known that as little as 2 eV is sufficient to break bonds (as a result of excited electrons⁴⁵). In this case a 1-MeV α particle would leave a nearly continuous trail of broken bonds and a 3-MeV α particle would break a bond, on the average, once every second atom distance along its path. Fleischer, Price and Walker⁴¹ have found from their unpublished work on polycarbonate resin that lower molecular weight polymers are attacked more rapidly by the appropriate etching solution than are higher weight polymers. Hence if one regards the region of broken bonds as having a very low molecular weight, it is reasonable to expect accelerated chemical attack there.

45. Bovey, F.A., The Effects of Ionizing Radiation on Natural and Synthetic High Polymers (Interscience Publishers, Inc., New York 1958) p. 16.

CHAPTER IV

EXPERIMENTAL

Equipment and Apparatus

The equipment and apparatus used may best be described according to its function in the registration of nuclear particle tracks in film, that is: exposure, development and identification.

Exposure

The production of the nuclear particles was accomplished by neutron activation - bombardment of target nuclei by neutrons - the neutrons being produced by a neutron generator. This work utilized the existing neutron generator facility at the Louisiana State University Nuclear Science Center. The generator is of the Cockcroft-Walton type originally built by Texas Nuclear Corporation and modified by Accelerators, Inc. The generator as used in this work produces a nearly isotropic yield of approximately 14 MeV neutrons from the following reaction.⁴⁶



The reaction may be written in shorthand notation as $\text{T}(d,n){}^4\text{He}$.

The main components of the generator are: a high vacuum system, an ion source, an in-line accelerating tube, water-cooled target assembly, high voltage supply, and a remote control console.⁴⁷

46. J. T. Prud'homme, Texas Nuclear Corporation Neutron Generators, (2nd ed., Texas Nuclear Corp., Austin, Texas, 1964) pp. 3-8

47. Ibid., pp. 13-54.

During operation, the deuterium ions (deuterons: ${}^2_1\text{H}^+$) are accelerated through a potential drop of 150 KV. Upon leaving the accelerating field, the deuterons strike the target, which in this work consisted of tritium (${}^3_1\text{H}$) absorbed in a layer of titanium which is evaporated onto a 0.010-inch thick copper backing.

The rated neutron yield of the generator is 1.2×10^{11} n/sec at 1.0 milliampere of beam current and 150 KV bombarding voltage which corresponds to a maximum usable neutron flux of 1.2×10^{10} n/cm²/sec at the target area. However, the neutron output decreases with time since the tritium in the target is depleted by the $\text{T}(d,n){}^3\text{He}$ reaction.⁴⁸

There were two types of films utilized to record the presence of nuclear particles -- a cellulose nitrate film manufactured by Kodak and a cellulose acetate butyrate film manufactured by Read Plastics.⁴⁹ The cellulose nitrate film, designated by Kodak as Type 106-01, is a nonphotographic detector capable of recording strongly ionizing radiations (protons, alpha particles, fission fragments, etc., directly and neutrons indirectly) in the presence of weakly ionizing radiations (light, x-rays, gamma rays, beta rays, etc.). The film consists of a thin coating of unsensitized, high-purity cellulose nitrate (8 to 10 microns thick) on one side of a 4-mil ESTAR polyester support. It is the cellulose nitrate coating that undergoes a structural change when the film is exposed to high specific ionization particles. The protons and alpha particles were produced by direct nuclear interactions with the nitrogen and oxygen in the cellulose nitrate emulsion.

48. Ibid., pp. 55-56.

49. Located in Rochville, Maryland.

The interactions considered were the fast neutron ${}^{16}_8\text{O} + {}^1_0\text{n} \rightarrow {}^{13}_6\text{C} + {}^4_2\alpha$ reaction and the thermal neutron ${}^{14}_7\text{N} + {}^1_0\text{n} \rightarrow {}^1_1\text{p} + {}^{14}_6\text{C}$ reaction⁵⁰ with cross-sections of 300 millibarns and 1.8 barns respectively. The cellulose nitrate film was also used to detect the presence of fission fragments produced from the interaction of uranium foils with fast and thermal neutrons.

The cellulose acetate butyrate film manufactured by Read Plastics is an extruded-colorless sheet with a thickness of .010 inches. Its response to fission fragments was compared to the cellulose nitrate.

A thermal neutron environment was produced by shielding the film to be exposed by at least four inches of paraffin in all directions.⁵¹ A substantially fast neutron environment was produced by placing the film adjacent the generator snout (target area). However, a 100% fast environment could not be assured due to neutron scatter and thermalization in the water cooling.

To aid in placement and exposure the pieces of film were cut to a size to be compatible with cardboard slide mounts. The film was inserted in the mounts which enabled the film to be easily handled and positioned. When uranium foils were utilized, they were positioned over the film and taped to the cardboard mounts with as little adhesion as possible to the film.

50. Personal communication with Mr. B. Stephen Carpenter of the Bureau of Standards on October 22, 1971.

51. Barry E. Chernick, Neutron Radiography - Utilization of Neutron From a Cockcroft-Walton Accelerator, Louisiana State University Mechanical Engineering Department Thesis, January, 1966

A relative measurement of the exposure was obtained by the use of an Eberline portable neutron rem counter (Model PNR-4) placed in the "exposure tunnel" during each experimental run. The PNR-4 is a portable, battery operated instrument having a 9-inch diameter, cadmium loaded, polyethylene sphere with a BF_3 tube in the center. According to the manufacturer, it has a response which closely follows the theoretical dose from neutrons over the energy range from .025 ev (thermal) to about 10 MeV. In order to obtain a digital response, an aural monitoring plug on the front panel was connected to a scaler mounted in the same equipment bin as the dose rate meter. During the first few weeks of research a second detector, a Texas Nuclear (Model 9140) NEMO dosimeter, was used outside the "exposure tunnel" in order to corroborate the measurements. The Model 9140 has a ^6LiI (Eu) crystal surrounded by a 10-inch sphere of polyethylene which is connected to an AC operated scaler. However, the Model 9140 became unreliable and its use was discontinued.

Figure VI is a top view of the Neutron Generator Facility at the Louisiana State University Nuclear Science Center showing the "exposure tunnel" and the positions of the Model PNR-4 and Model 9140 detectors.

Development

The exposed films were removed from the cardboard holders and marked so as to be able to identify the film after its "development". The films were "developed" (in reality the films are being etched) in a 6.5 N NaOH solution at 57° C for 3.5 minutes for the cellulose nitrate film, and at 49° C for 45 minutes for the cellulose

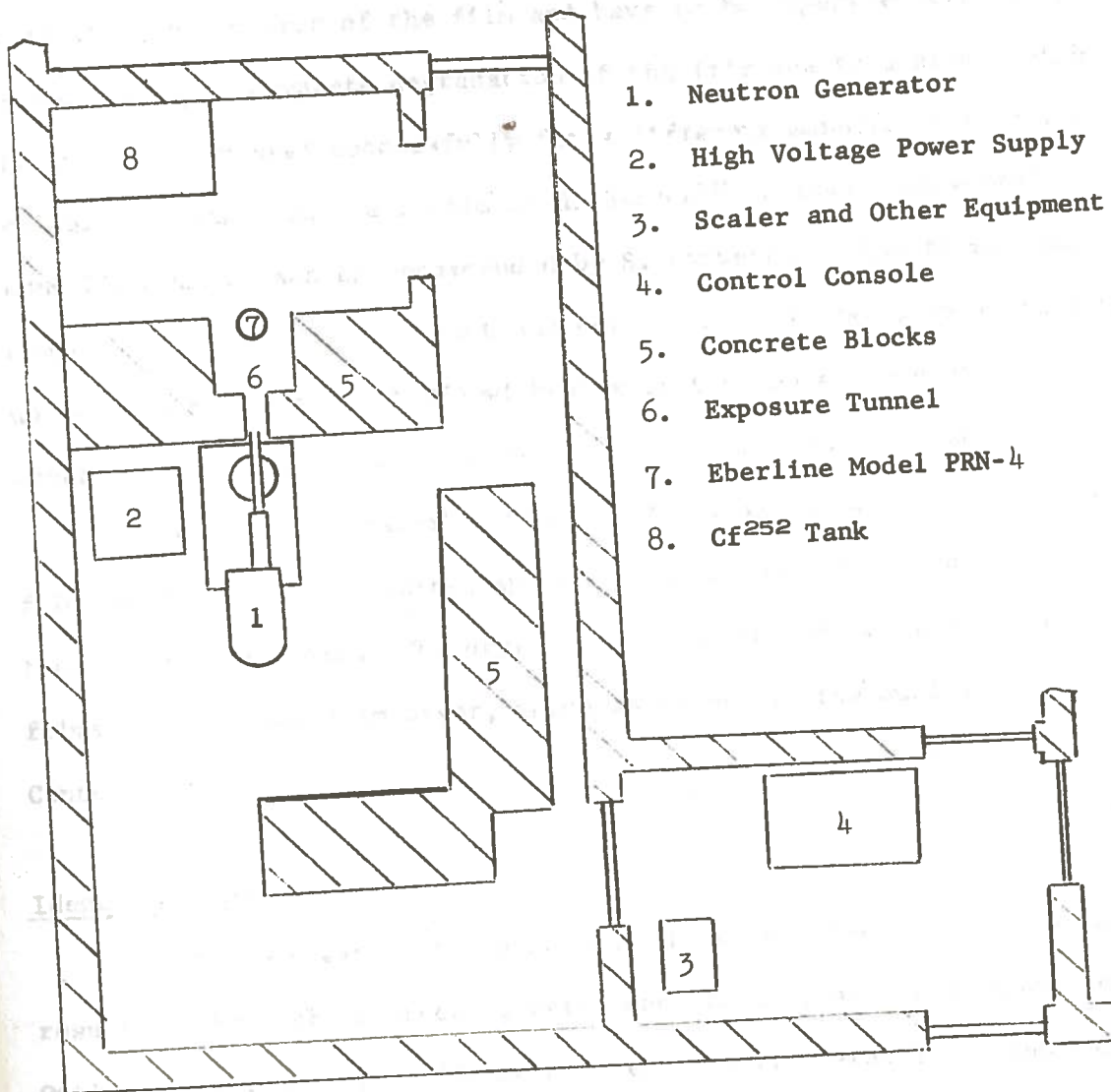


Figure VI. Neutron Generator Facility at the Louisiana State University Nuclear Science Center

acetate butyrate film. Etching of the cellulose nitrate film is a more-or-less trial and error technique since different pieces of cellulose nitrate from the same sheet will have different etch characteristics.⁵² The etch conditions for the cellulose acetate butyrate vary with the manufacturer of the film and have to be experimentally determined. After a complete degradation of the film due to a strong etch (which had been used successfully for a different manufacturer of the cellulose acetate butyrate film by H. Berger⁵³) a less severe etch condition was chosen as recommended by S. Carpenter. The films were completely immersed in the NaOH and periodically agitated so as to have uniform "development". A 250 ml beaker resting on a temperature controlled hot-plate provided the "developing pan and heat source".

After the prescribed time in the "developing" solution, the films were rinsed in running tap water for at least two minutes and then forced air dried. The drying was accomplished by hanging the films in the Kodak film dryer, which is in use in the Nuclear Science Center dark room.

Identification

The nuclear particle tracks, which have been enlarged as a result of the etching process, were identified by use of an American Optical Microstar Series 10 microscope. The microstar 10 is equipped with a high intensity illuminator which incorporates a built-in neutral

52. Carpenter, Op. Cit.

53. Berger, Harold, "Image Detection Methods for 14.5 MeV Neutrons: Techniques and Applications" (unpublished).

density filter. The Microstar 10 has a magnification potential of 970X but for the present experimental research a magnification of 430X was found to be adequate.

In order to preserve the image viewed through the microscope lens, an American Optical Model 682F Camera mounted above the microscope was used to make Polaroid prints. The Model 682F camera has various shutter speeds ranging from 1/100 sec to a Time setting. During the earlier stages of the research, Type 57 Polaroid film was used, but this had to be changed to Type 52 due to the unavailability of a new supply of the Type 57. Exposure calibrations were performed for each type of film and the shutter speeds determined -- 1/50 sec for Type 57 and 3/10 sec for Type 52. In order to establish the magnification appearing on the film was the same as that in the eyepiece (430X), a stage micrometer was obtained from the Microbiology Department of Louisiana State University and photographed. The photograph of the stage micrometer, Figure VII, shows that the magnification appearing on the film is indeed 430X.

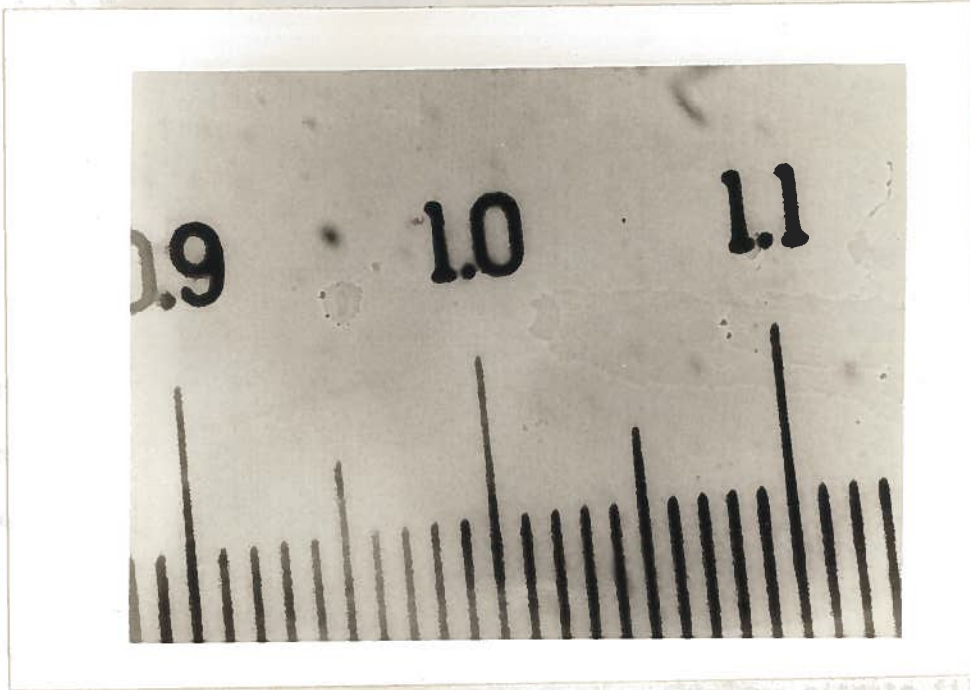


Figure VII. Photograph of a Staged Micrometer to Verify the Magnification of the Microscope at 430X

Figure VII is a photograph of the negative nitrate film magnified 430X. This region contains the uranium foil. This region contains the uranium foil fragment tracks. (This region will be photographed later.)

Figure VIII is a photograph of the negative nitrate film showing the region of the uranium foil. The uranium foil was mounted. Again, this region contains the uranium foil fragment tracks, but the tracks are more dense than in the preceding figure due to the presence of an abundance of uranium foil fragment tracks.

Figure IX is a photograph showing the interface of the uranium foil area and the remainder of the film. Upon close

14. All of the photographs were produced with a magnification of 430X and this factor is to be applied in all subsequent photographs.

CHAPTER V

Results

A number of unsuccessful attempts were made to achieve the operating conditions necessary to register nuclear particle tracks in the film. The first attempts involved only the cellulose nitrate film, which appears to be the most sensitive to alphas and protons. After four unsuccessful attempts, the tracks pictured in Figures VIII, IX, and X were recorded using a uranium foil mounted on the cellulose nitrate film. The film was exposed to a fast neutron environment for five minutes with the neutron generator operating at 150 KV and 1.4 ma beam current giving a total count of 779,000 on the Eberline Model PRN-4 detector. The films were etched for 4 minutes in the 6.5N NaOH solution at 57° C.

Figure VIII is a photograph of the cellulose nitrate film magnified 430X⁵⁴ showing a region of the film to the side of the uranium foil. This region contains alpha tracks, proton tracks and stray fission fragment tracks. (These tracks will be distinguished later.)

Figure IX is a photograph of the cellulose nitrate film showing the region of the film where the uranium foil was mounted. Again, this region contains proton, alpha and fission fragment tracks but the tracks are more dense than in the preceding figure due to the presence of an abundance of fission fragment tracks.

Figure X is a photograph attempting to show the interface of the uranium foil area and the remainder of the film. Upon close

54. All of the photographs were produced with a magnification of 430X and this factor is to be assumed in all subsequent photographs.

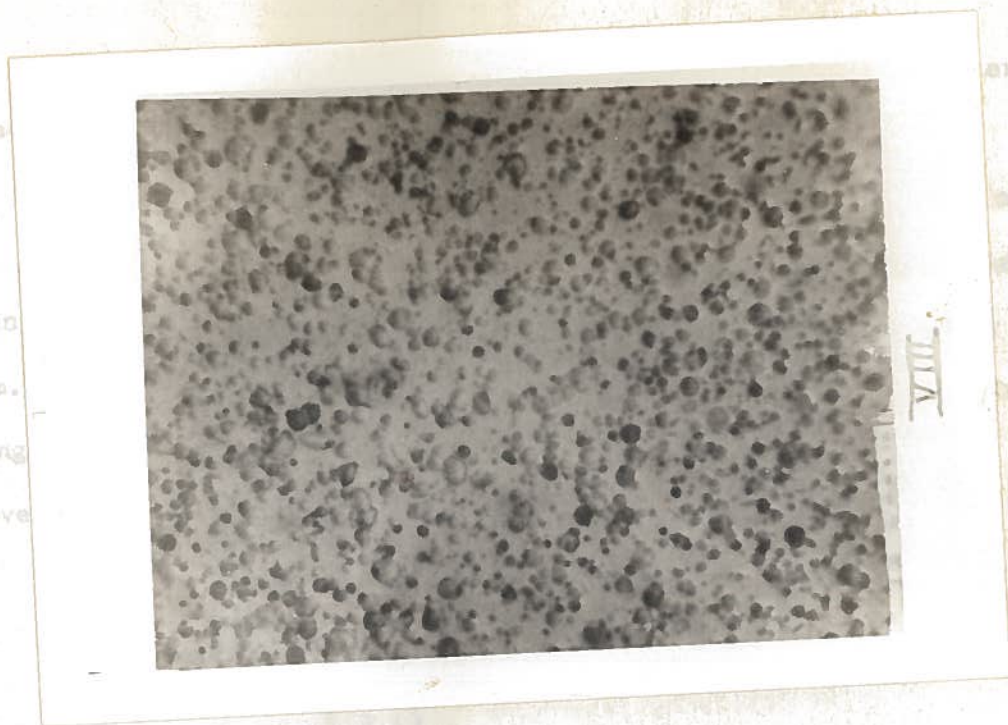


Figure VIII. Photograph of Cellulose Nitrate Film Exposed to a Fast Neutron Flux Shown in the Region to the Side of the Uranium Foil Placement

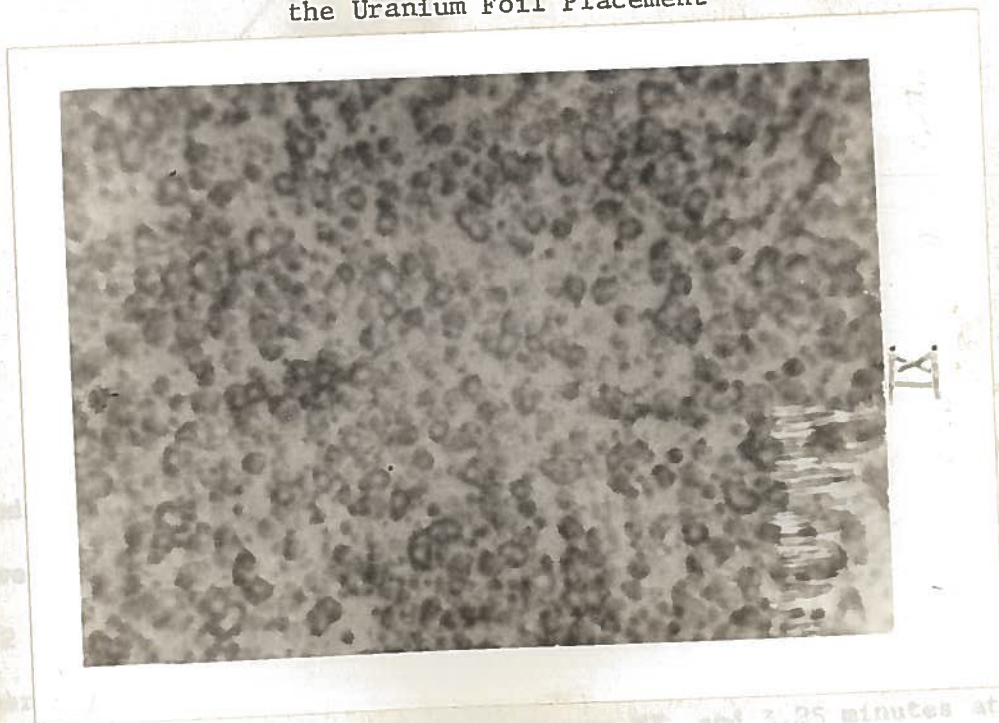
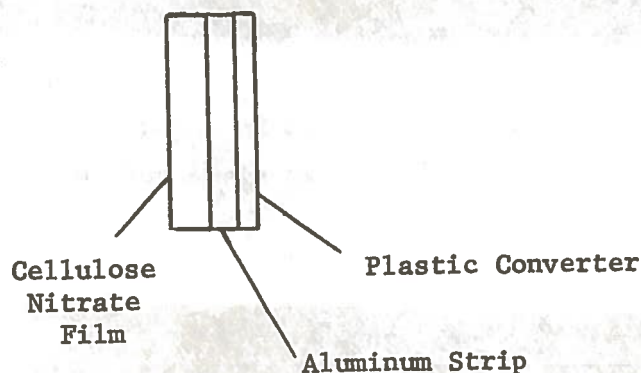


Figure IX. Photograph of Cellulose Nitrate Film Exposed to a Fast Neutron Flux Beneath the Uranium Foil

inspection one can see the density of the tracks change as the interface is crossed.

Figures XI, XII, XIII, XIV and XV show the results obtained in an attempt to reduce the number of proton tracks recorded on the film. A reduction in the number of proton tracks was attempted by using a sandwich arrangement depicted below consisting of a plastic converter, aluminum strips and the cellulose nitrate film.



The films were exposed to a neutron environment so as to produce protons in the plastic converter. The films were exposed for five minutes each with the neutron generator operating at 150 KV and 1.2 beam current giving a total count of approximately 2.2×10^6 on the Eberline Model PRN-4 detector. The films were etched for 3 minutes in a 5.6N NaOH solution at 59° C for Figure XI, and 3.25 minutes at 58° C for Figures XIV-XV.



Figure X. Photograph of Cellulose Nitrate Film Exposed to a Fast Neutron Flux Shown in the Uranium Foil-Film Interface



Figure XI. Photograph of Cellulose Nitrate Film Exposed to a Fast Neutron Flux for Use as a Basis for Flux Reduction Determination

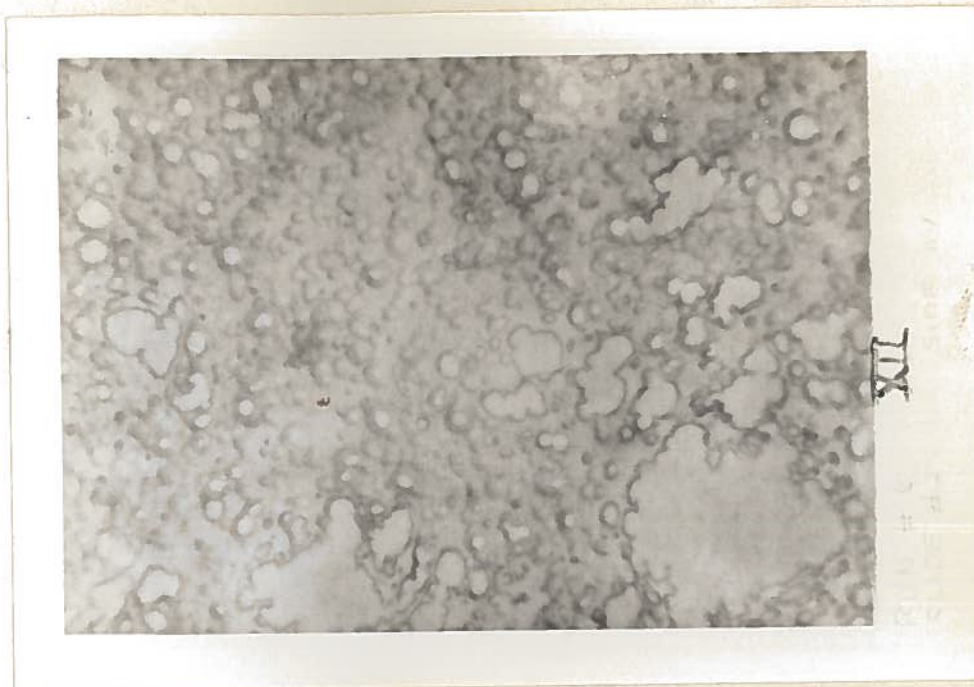


Figure XII. Photograph of Cellulose Nitrate Film Exposed to a Fast Neutron Flux with one Sheet of Aluminum Covering for Particle Flux Reduction (Accidentally Over-etched)

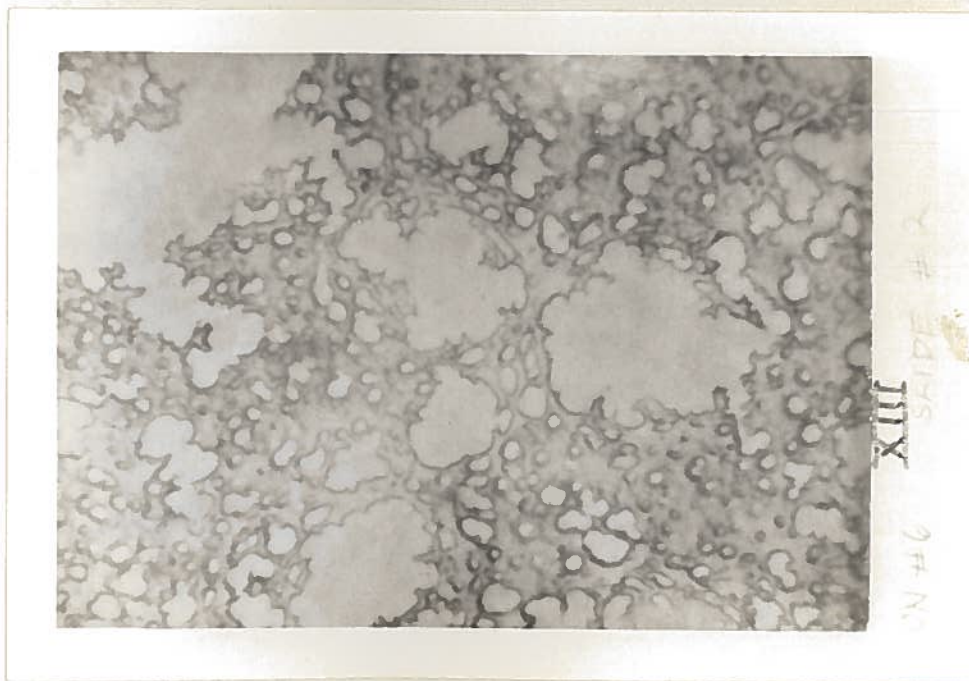


Figure XIII. Photograph of Cellulose Nitrate Film Exposed to a Fast Neutron Flux with Two Sheets of Aluminum Covering for Particle Flux Reduction (Accidentally Over-etched)

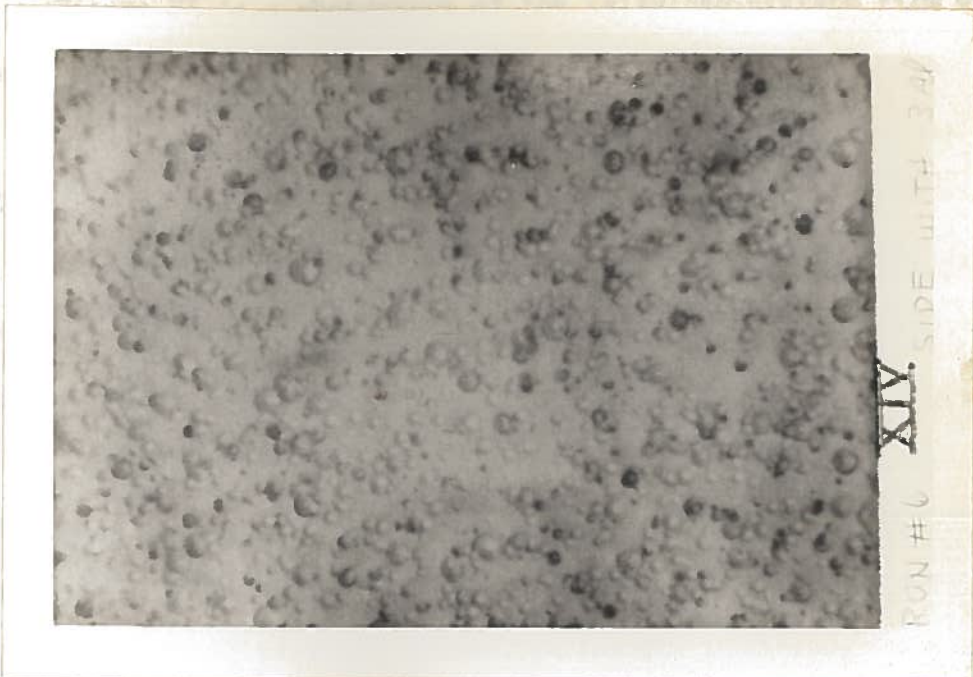


Figure XIV. Photograph of Cellulose Nitrate Film Exposed to a Fast Neutron Flux with Three Sheets of Aluminum Covering for Particle Flux Reduction

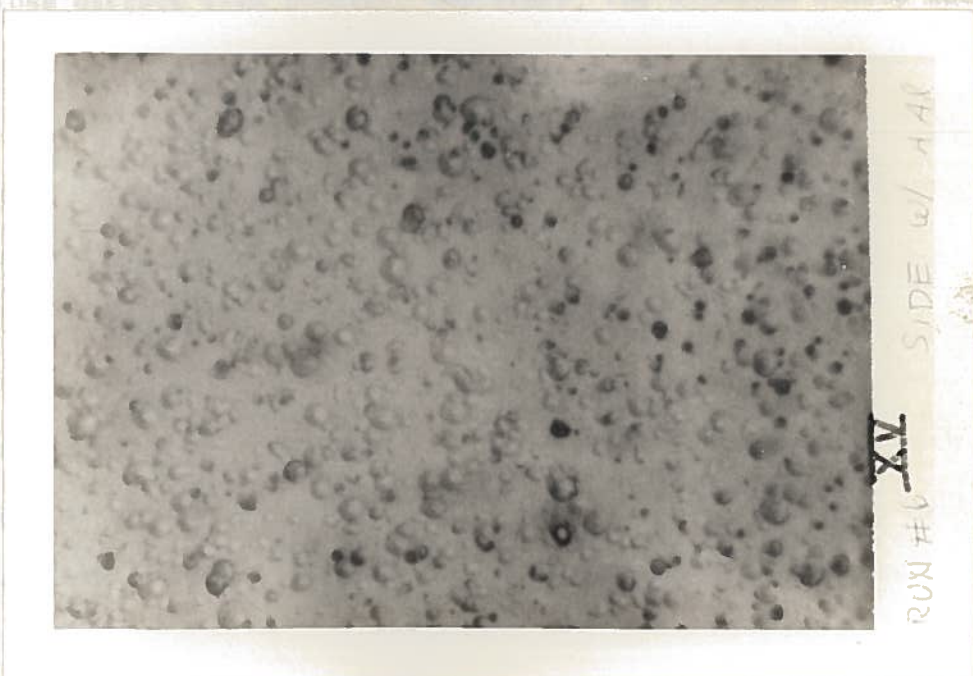


Figure XV. Photograph of Cellulose Nitrate Film Exposed to a Fast Neutron Flux with Four Sheets of Aluminum Covering for Particle Flux Reduction

Figure XI is a photograph of the cellulose nitrate film without the aluminum sheets in order to obtain a reference film for the amount of reduction. The photograph of the film shows the presence of both alpha and proton tracks in the film.

Figures XII and XIII contain one and two sheets of aluminum, respectively. However, no conclusions can be drawn from them due to the fact that they were inadvertently over-etched.

Figures XIV and XV contain three and four sheets of aluminum, respectively. Although there may be a slight reduction in the number of tracks from Figure XI to Figure XV, it is not conclusive. This may be due to a number of reasons. Since the thermal neutrons give the proton reaction, the fast neutrons present, which did not interact with the plastic converter, may have been thermalized and reacted with the cellulose nitrate film itself. Therefore, the aluminum sheets would have had no effect on these latter interactions. Another postulation would be the effect of qualitative measurements with the existing equipment instead of quantitative measurements. If more sophisticated measurement techniques could have been employed, a possible difference might have been noted.

Figures XVI through XIX show the results of an investigation into the response of cellulose nitrate and cellulose acetate butyrate to register the tracks produced from fast neutron activation and at the same time determine the neutron flux spacial distribution. Strips of cellulose nitrate and cellulose acetate butyrate were mounted adjacent to each other in slide holders and positioned in front of the beam. Four slides were used and each was rotated 90° from the other.

The slides were exposed for five minutes each with the neutron generator operating at 150 KV and 1.6 ma beam current giving a total count of 2.0×10^6 on the Eberline Model PRN-4 detector. The cellulose nitrate film was etched in 6.5N NaOH for 3.5 minutes at 57° C, while the cellulose acetate butyrate was etched for 45 minutes at 49° C. The sketch below shows the relation of the films to the generator snout.



Film shown
in Fig. XVI

Film shown
in Fig. XVII

Film shown
in Fig. XVIII

Film shown
in Fig. XIX

An investigation of Figures XVI-XIX indicates that there is no appreciable difference in the neutron flux distribution around the target area. However, the cellulose nitrate film does seem to have a higher response to the ionizing particles than the cellulose acetate butyrate as indicated by the greater number of "holes" formed in the cellulose nitrate.

No explanation can be given to account for the symmetrical distribution of "holes" in Fig. XVI(b) (the larger "holes" being surrounded by smaller "holes"), although it does resemble effects often produced when highly enriched uranium fission is recorded.⁵⁵

Figures XX and XXI are the results of an attempt to distinguish between the alpha and proton tracks recorded in the cellulose nitrate. Both were exposed for five minutes with the neutron generator operating at 150 KV and 1.6 ma beam current. Figure XX was a fast

55. Courtney, J., Assistant Professor, Louisiana State University Nuclear Science Center. Personal conversation on November 11, 1971

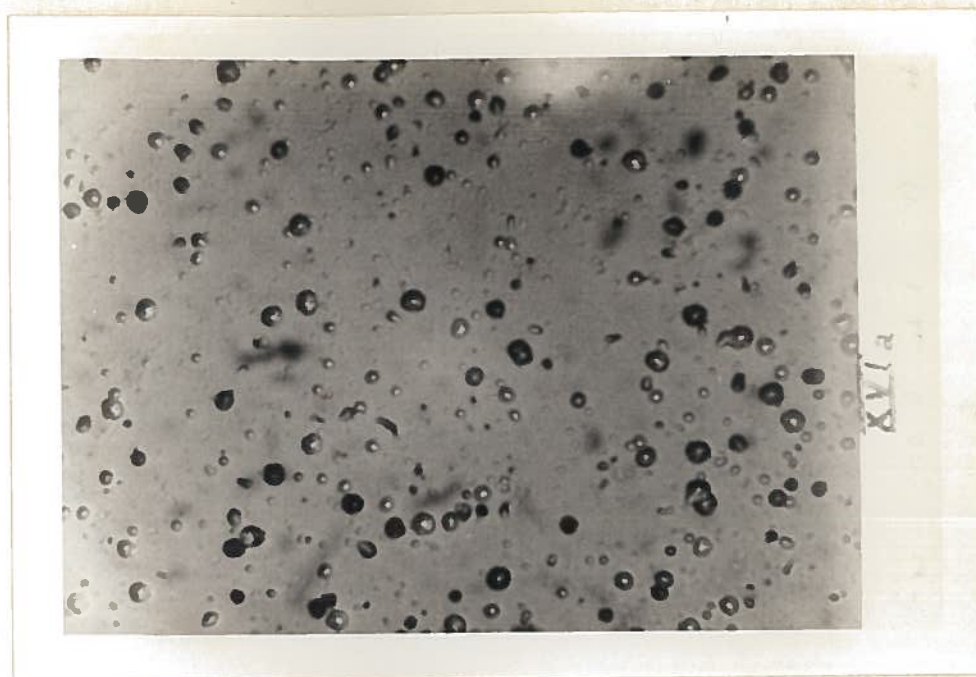


Figure XVI(a). Photograph of Cellulose Nitrate Film Exposed to
Fast Neutron Flux. Bottom Plate

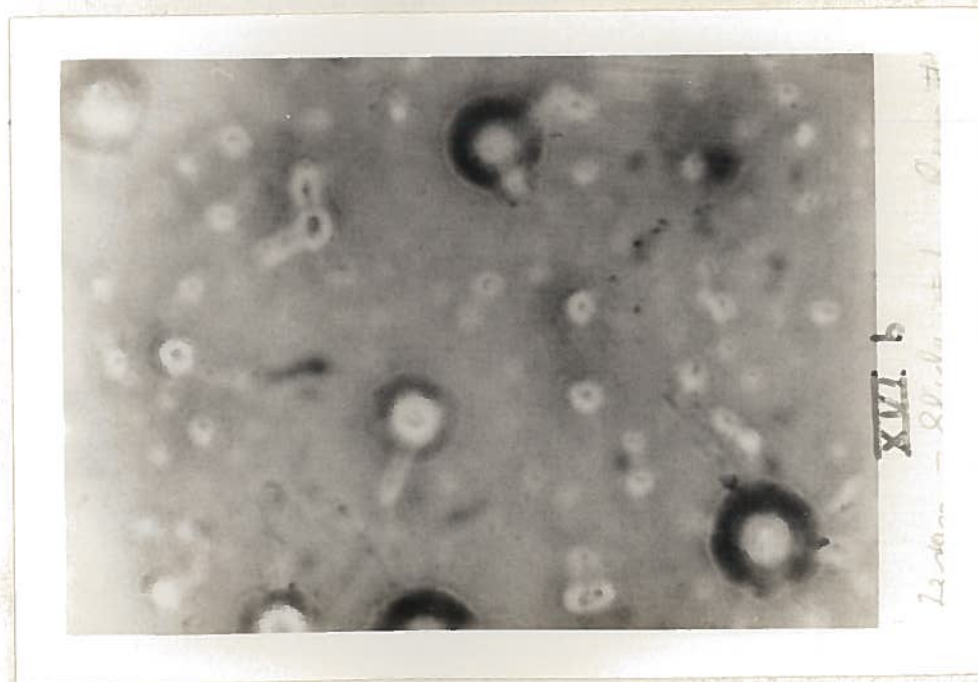


Figure XVI(b). Photograph of Cellulose Acetate Butyrate Film
Exposed to a Fast Neutron Flux. Top Plate

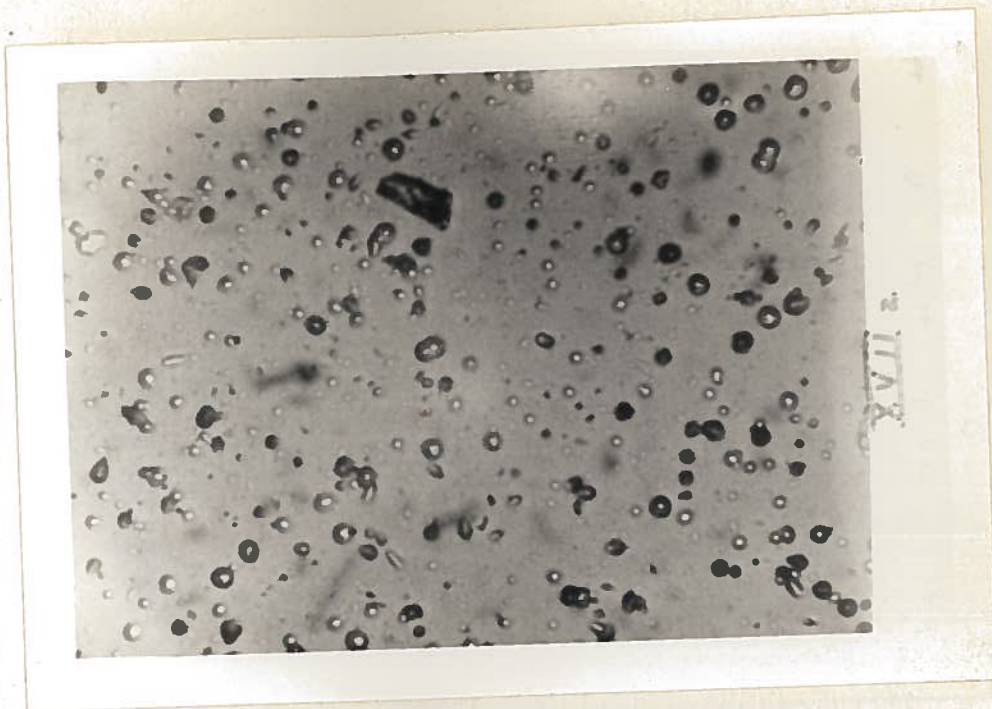


Figure XVII(a). Photograph of Cellulose Nitrate Film Exposed to a Fast Neutron Flux. Right Plate

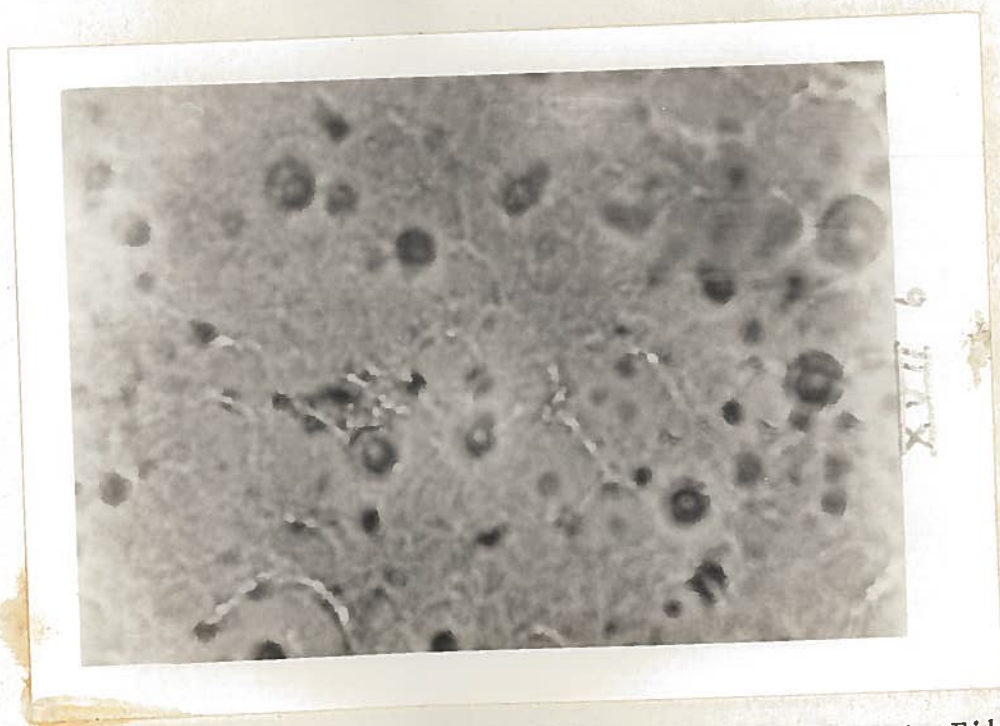


Figure XVII(b). Photograph of Cellulose Acetate Butyrate Film Exposed to a Fast Neutron Flux. Left Plate

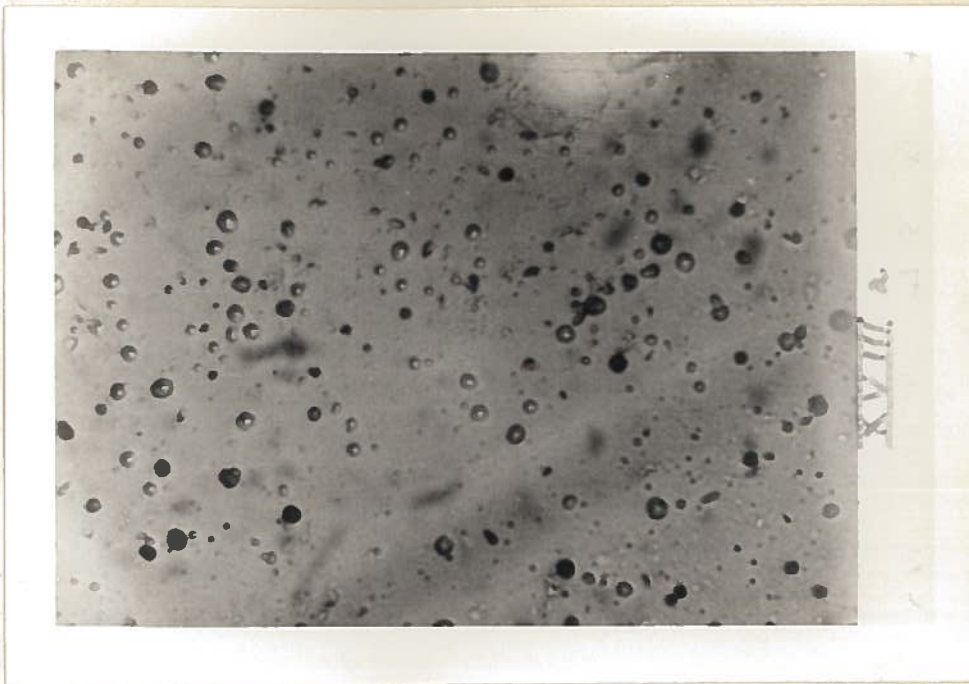


Figure XVIII(a). Photograph of Cellulose Nitrate Film Exposed to a Fast Neutron Flux. Top Plate



Figure XVIII(b). Photograph of Cellulose Acetate Butyrate Film Exposed to a Fast Neutron Flux. Bottom Plate

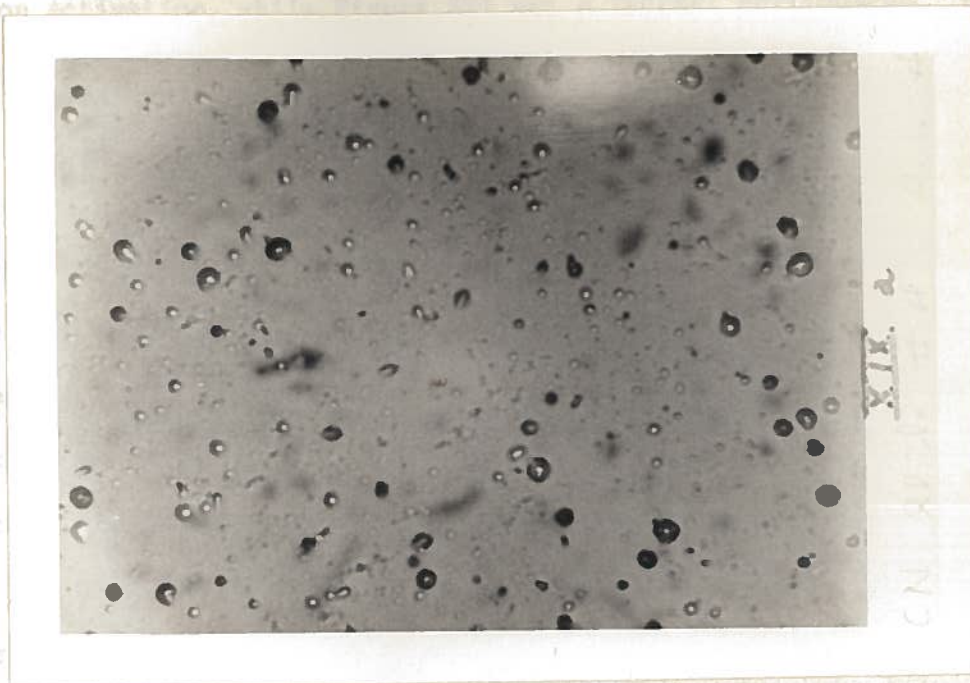


Figure XIX(a). Photograph of Cellulose Nitrate Film Exposed to a Fast Neutron Flux. Left Plate

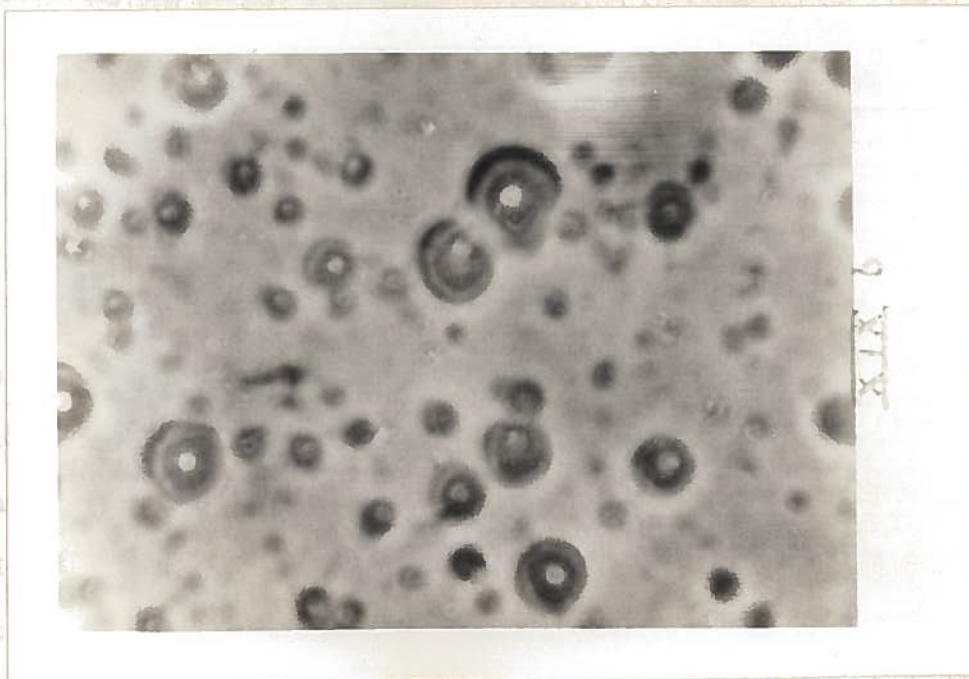


Figure XIX(b). Photograph of Cellulose Acetate Butyrate Film Exposed to a Fast Neutron Flux. Right Plate

neutron activation, while Figure XXI was a thermal environment. Etching was performed in 6.5N NaOH for 3.5 minutes at 57° C.

An investigation of the figures reveals that there is a difference between the tracks produced by alpha particles and the ones produced by protons. Figure XX contains both alpha and proton tracks, while Figures XXI contains primarily proton tracks. The alphas appear to leave larger and less densely populated tracks while the proton tracks are small and highly concentrated due to the higher cross-section for the proton reaction.

Figures XXII-XXV show the results of an attempt to determine the relative responsiveness of cellulose nitrate and cellulose acetate butyrate to fission fragments. Figures XXII and XXIII are photographs of the areas of the cellulose nitrate and cellulose acetate butyrate respectively in direct contact with freshly cleaned⁵⁶ uranium foils exposed to fast neutron fluxes, which gave a total count of 230,000 for the cellulose nitrate and 150,000 for the cellulose acetate butyrate on the Eberline Model PRN-4. The cellulose nitrate was etched in 6.5N NaOH for 3.5 minutes at 57° C while the cellulose acetate butyrate was etched for 40 minutes at 50° C. The tracks found on the cellulose nitrate film are a combination of protons, alphas and fast fission fragments, while those formed on the cellulose acetate butyrate film are a combination of alphas and fast fission fragments only. Figures XXII(a) and XXIII(a) show the same film in an area outside the point of foil placement. Upon comparing the same type of film in different areas, one can

56. A previous attempt (not detailed in this work) was unsuccessful for the cellulose acetate butyrate, possibly due to oxidized foils.

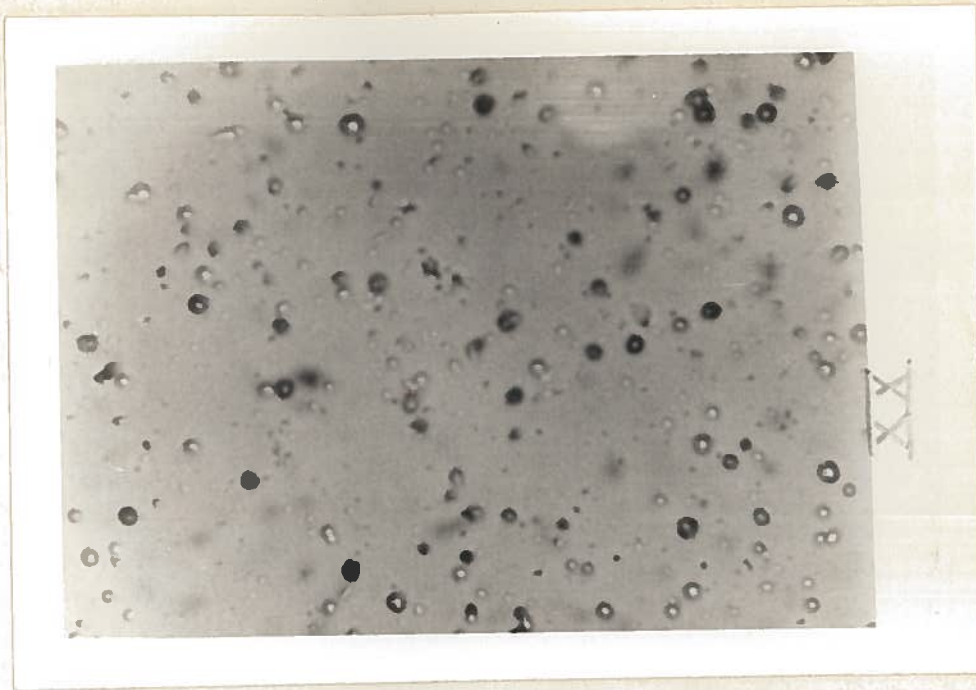


Figure XX. Photograph of Cellulose Nitrate Film Exposed to a Fast Neutron Flux in Order to Produce Both Alpha and Proton Tracks

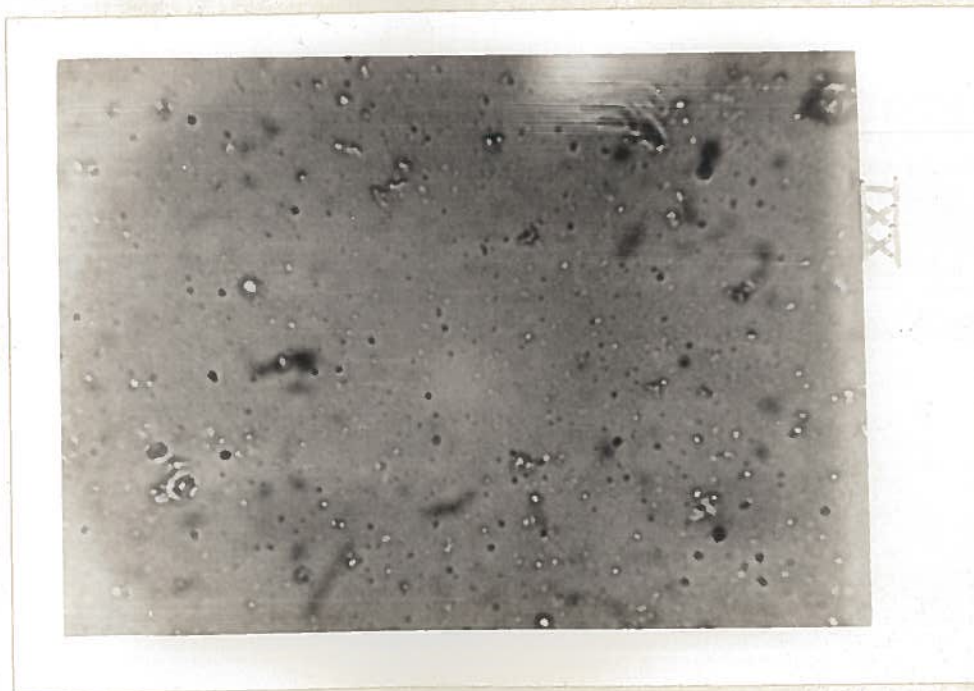


Figure XXI. Photograph of Cellulose Nitrate Film Exposed to a Thermal Neutron Flux in Order to Eliminate Alpha Track Production

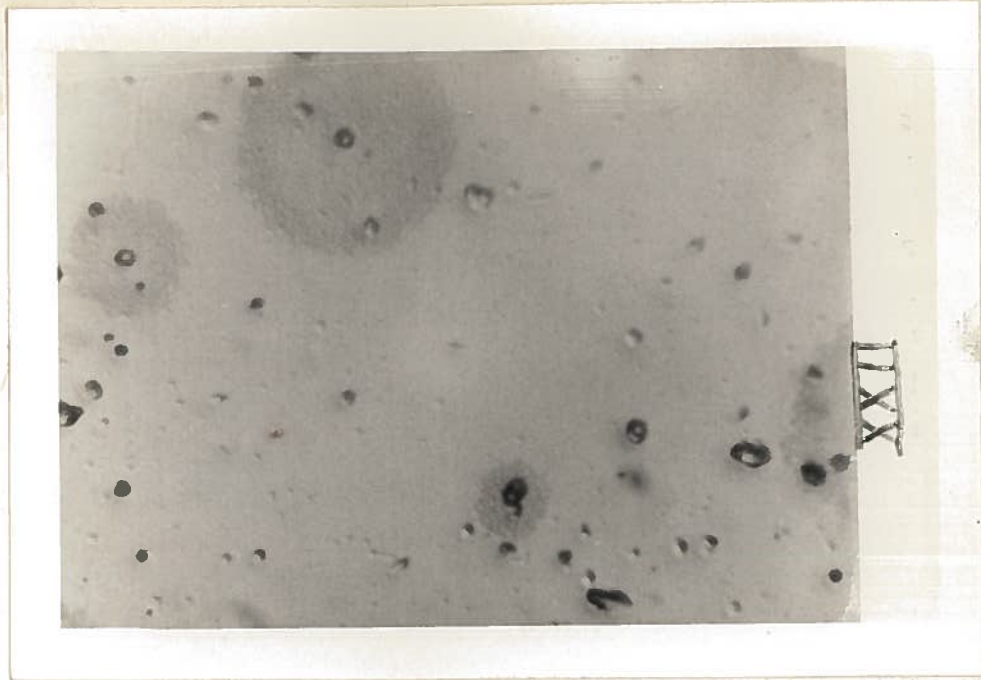


Figure XXII. Photograph of Cellulose Nitrate Film Exposed to a Fast Neutron Flux Beneath the Uranium Foil



Figure XXIII. Photograph of Cellulose Acetate Butyrate Film Exposed to a Fast Neutron Flux Beneath the Uranium Foil

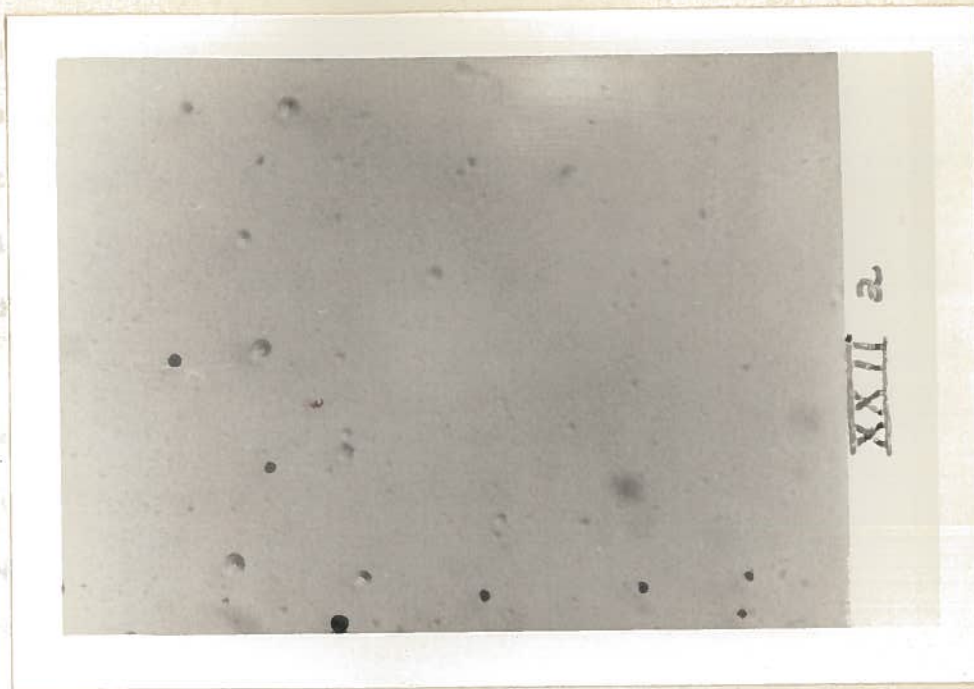


Figure XXII(a). Photograph of Cellulose Nitrate Film Exposed to a Fast Neutron Flux Showing the Region to the Side of the Uranium Foil Placement

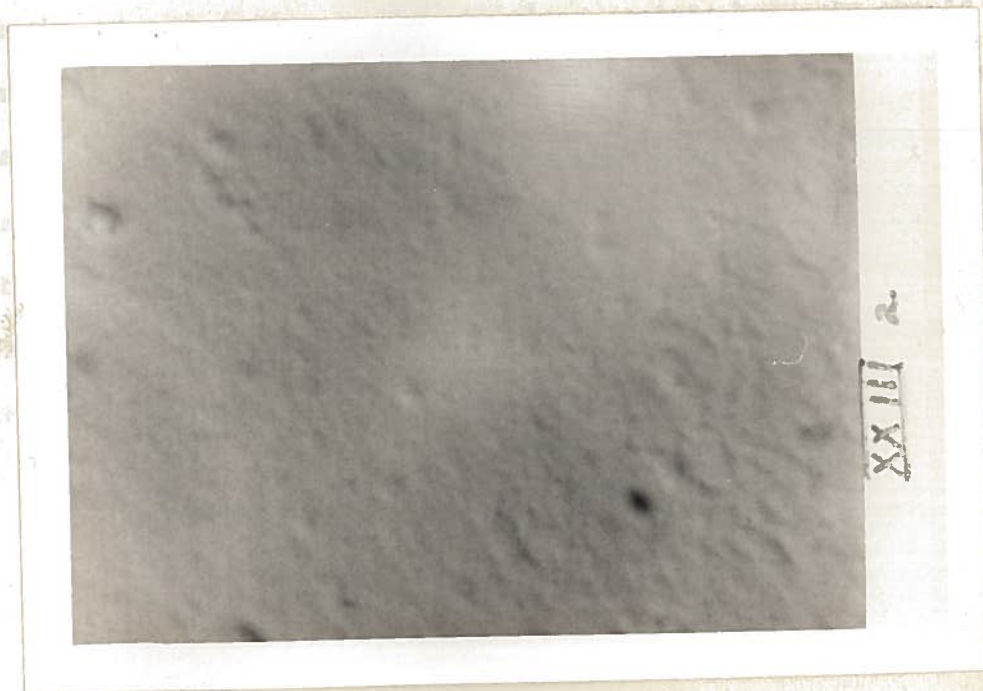


Figure XXIII(a). Photograph of Cellulose Acetate Butyrate Film Exposed to a Fast Neutron Flux Showing the Region to the Side of the Uranium Foil Placement

determine the size and shape of the fast fission fragment track. Upon further comparison of the two types of film one is able to conclude that the cellulose nitrate film's response to fast fission fragments is not significantly greater than the cellulose acetate butyrate. However, the alpha response of the cellulose nitrate is appreciably greater.

Figures XXIV and XXV are photographs of the cellulose nitrate and cellulose acetate butyrate film, respectively, in the area of uranium foil contact which were exposed to thermal neutron fluxes, giving total counts of 132,000 for the cellulose nitrate and 176,000 for the cellulose acetate butyrate on the Eberline Model PRN-4. The same etching technique was used as that on the previous film. The tracks found on the cellulose nitrate film are a combination of protons and thermal fission fragments (with the possibility of some alpha decay) while the ones appearing on the cellulose acetate butyrate should be thermal fission fragments alone (also with the possibility of some alpha decay). Figures XXIV(a) and XXV(a) show the same film outside the area of foil placement. Upon comparison of the two separate areas of the same film and a comparison of the two different films, one can conclude the response to thermal fission fragments appears to be greater in the cellulose nitrate than in the cellulose acetate butyrate.

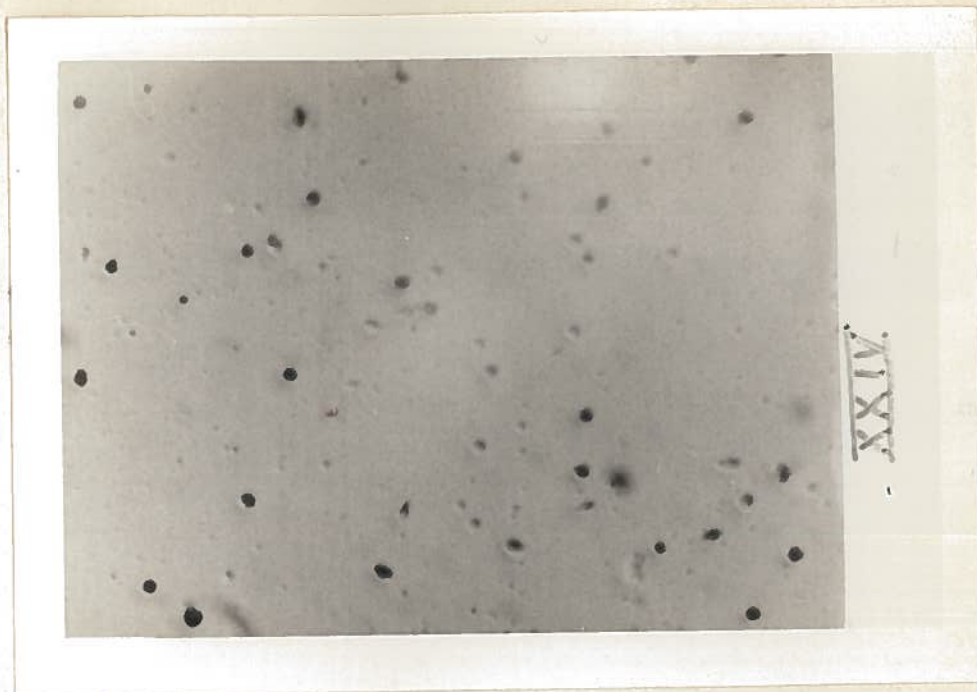


Figure XXIV. Photograph of Cellulose Nitrate Film Exposed to a Thermal Neutron Flux Beneath the Uranium Foil



Figure XXV. Photograph of Cellulose Acetate Butyrate Film Exposed to a Thermal Neutron Flux Beneath the Uranium Foil

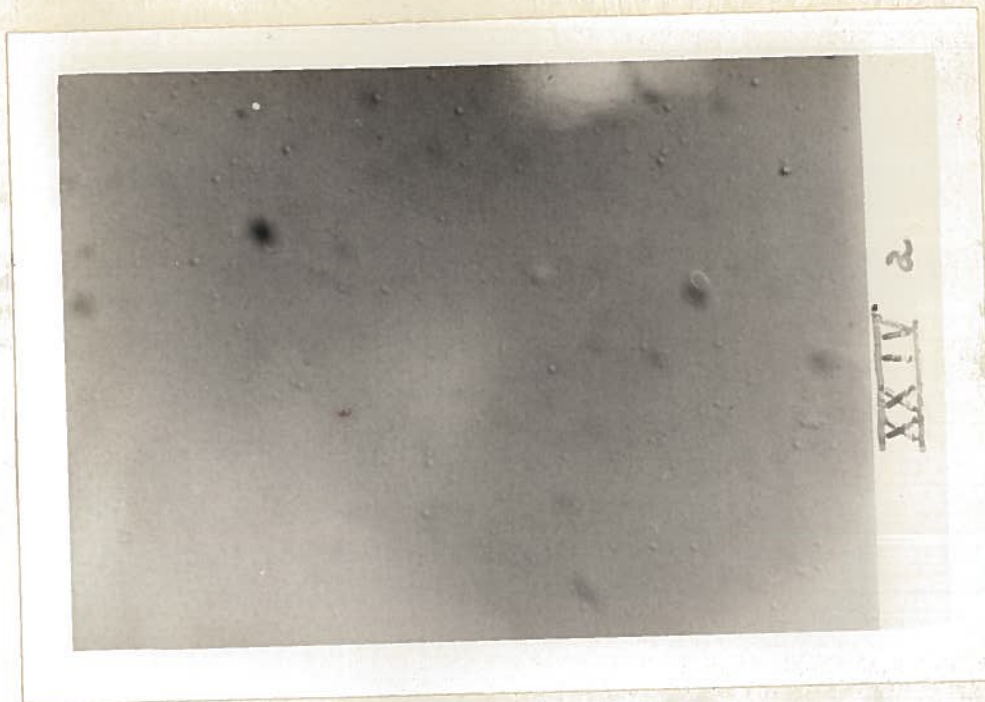


Figure XXIV(a). Photograph of Cellulose Nitrate Film Exposed to a Thermal Neutron Flux Showing the Region to the Side of the Uranium Foil Placement

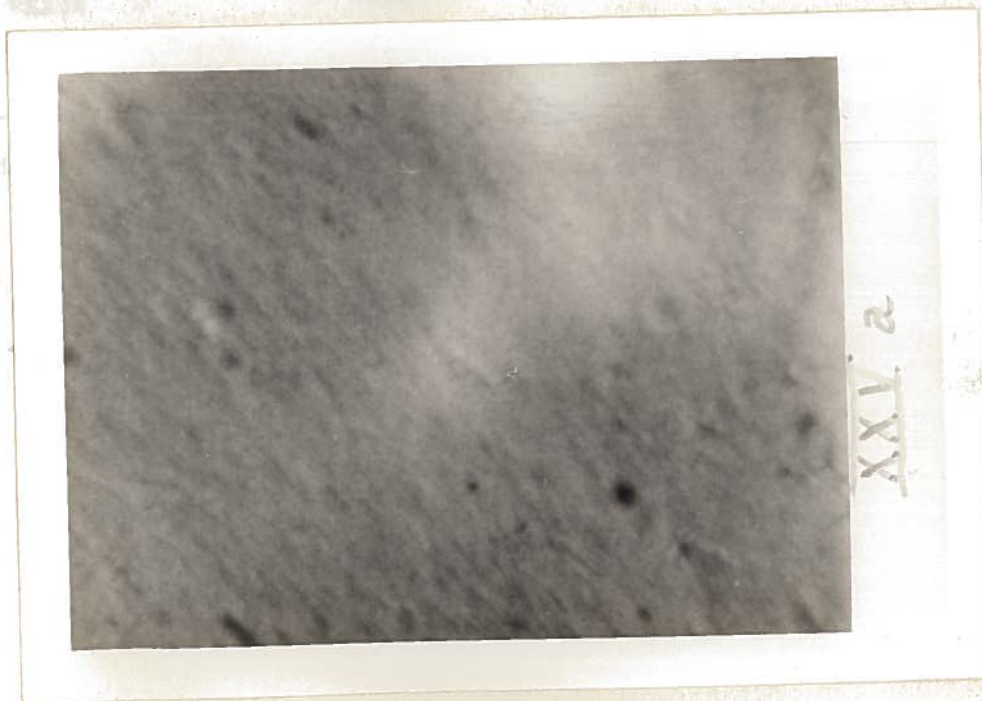


Figure XXV(a). Photograph of Cellulose Acetate Butyrate Film Exposed to a Thermal Neutron Flux Showing the Region to the Side of the Uranium Foil Placement

TABLE 8

EXPOSURE VALUES

Photograph Number (Figure Number)	Neutron Generator		Time (min)	Total Count
	Operating Voltage kv	Beam Current ma		
VIII-X	150	1.4	5	779,000
XI-XV	150	1.2	5	2,250,000
XVI-XIX	150	1.6	5	2,000,000
XX	150	1.6	5	not used
*XXI	150	1.6	5	not used
XXII	150	1.4	1	230,000
XXIII	150	1.4	2	150,000
*XXIV	150	1.4	2	132,000
*XXV	150	1.4	2	176,000

*Indicates a thermal neutron environment.

TABLE 9

DEVELOPING TECHNIQUES

Photograph Number (Figure Number)	Etching Solution	Etching Solution Temperature (°C)	Etch Time (min)
VIII-X	6.5N NaOH	57	4
XI	6.5N NaOH	59	3
XII-XIII	6.5N NaOH	58	3.25*
XIV-XV	6.5N NaOH	58	3.25
XVI-XIX (a)	6.5N NaOH	57	3.5
XVI-XIX (b)	6.5N NaOH	49	45
XX-XXI	6.5N NaOH	57	3.5
XXII and XXIV	6.5N NaOH	57	3.5
XXIII and XXV	6.5N NaOH	50	40

*May have been a timing error

CHAPTER VI

CONCLUSIONS AND RECOMMENDATIONS

Conclusions

This investigation demonstrates that nuclear particle tracks can be detected and distinguished by the use of special film coatings on a polyester base. The results obtained as to the sensitivity of the two film specimens under consideration follow the theoretical predictions that the cellulose nitrate film is more sensitive than the cellulose acetate butyrate. The cellulose nitrate film was able to record particles as light as protons while the cellulose acetate butyrate was limited to alpha and fission fragment tracks.

The sensitivity and ease of developing would make the cellulose nitrate film most desirable in particle track recording for a variety of purposes. These would include detection film badges, fissionable composition analysis and neutron radiography.

Recommendations

Further study and evaluation would be useful in the following areas:

1. Investigation of the sensitivity of various other recording films and media. This could include a number of other materials, such as Mica and soda glass, mentioned in earlier papers. From further investigation a sensitivity listing could be confirmed and the most economical method of track registration for a particular purpose selected.
2. With the use of more sophisticated detection and analyzing techniques the depth of particle penetration could be determined, and

from this a back calculation could be performed to determine the initial energy. A calibration of depth of penetration versus the initial energy would lead to a more desirable neutron detector than the present film badge.

3. A foreseeable use of the track-etch technique would be in the production of biological filters with equally spaced uniform holes. According to the research team of R. Fleischer, P. Price and R. Walker:

"Because of the random positions of the holes, the fraction of the filter surface which is open cannot exceed about 2 percent without some overlap of holes. With increasing porosity the efficiency of a filter in separating particles of closely similar size is impaired."⁵⁷

Uniform distribution may be accomplished with the use of a variety of grids of sufficient thickness to prevent particle penetration. The grids could be orientated in relation to each other so as to provide an opening sufficiently large enough to allow passage of one particle. In this manner the particles could be evenly and uniformly spaced. With sufficient information on hole size as a function of etch time the proper hole could be produced for its intended use.

4. Additionally, there are many other areas that have been proposed by members of the faculty which should prove fruitful.

57. Fleischer, R. L., P. B. Price, E. M. Symes, "Novel Filters for Biological Materials," Science, 143, 249 (1964).

VITA

Michael T. Pulaski was born on July 18, 1945, in Dallas, Texas.

Upon graduating from Houston High School, Houston, Mississippi, May, 1963, he entered the United States Air Force Academy in June of the same year. In January, 1965, he entered Louisiana State University, Baton Rouge, where he received the degree of Bachelor of Science in Mechanical Engineering in May, 1968. He then entered the Law School and Graduate School of Louisiana State University in September of 1968, pursuing a Juris Doctor degree in the Law School and a Master of Science degree in the Department of Nuclear Engineering.

In December of 1971, he received the degree of Juris Doctor from the Louisiana State University Law School. At present he is a candidate for the degree of Master of Science in Nuclear Engineering.